# Chaotic Behavior of Multidimensional Hamiltonian Systems: Disordered lattices, granular chains and DNA models


**Haris Skokos**

**Department of Mathematics and Applied Mathematics**
**University of Cape Town**
**Cape Town, South Africa**

**E-mail: haris.skokos@uct.ac.za**
**URL: http://math_research.uct.ac.za/~hskokos/**



**Work supported by the UCT Research Committee**

# Outline

**The quartic disordered Klein-Gordon (DKG) model and the disordered discrete nonlinear Schrödinger equation (DDNLS)**

- Different dynamical behaviors
- Lyapunov exponents
- Deviation Vector Distributions (DVDs)

**Chaotic behavior of granular chains (coexistence of smooth and non-smooth nonlinearities)**

- Do granular nonlinearities and the resulting chaotic dynamics destroy energy localization? If yes, how?
- Comparison with the disordered Fermi-Pasta-Ulam-Tsingou (FPUT) model

**The Peyrard-Bishop-Dauxois (PBD) model of DNA**

- Lyapunov exponents and different dynamical regimes
- Behavior of DVDs
- Effect of heterogeneity on system's chaoticity

**Future works - Summary**

# The
# DKG and DDNLS
# models

# Work in collaboration with

**Bob Senyange (PhD student): DKG model**

**Bertin Many Manda (PhD student): DDNLS model**

# Interplay of disorder and nonlinearity

Waves in disordered media – Anderson localization [Anderson, Phys. Rev. (1958)]. Experiments on BEC [Billy et al., Nature (2008)]

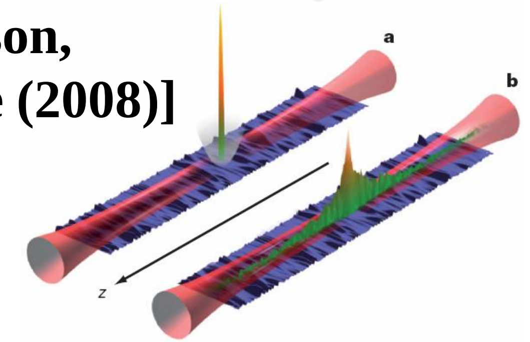


Waves in nonlinear disordered media – localization or delocalization?

Theoretical and/or numerical studies [Shepelyansky, PRL (1993) – Molina, Phys. Rev. B (1998) – Pikovsky & Shepelyansky, PRL (2008) – Kopidakis et al., PRL (2008) – Flach et al., PRL (2009) – S. et al., PRE (2009) – Mulansky & Pikovsky, EPL (2010) – S. & Flach, PRE (2010) – Laptyeva et al., EPL (2010) – Mulansky et al., PRE & J.Stat.Phys. (2011) – Bodyfelt et al., PRE (2011) – Bodyfelt et al., IJBC (2011)]

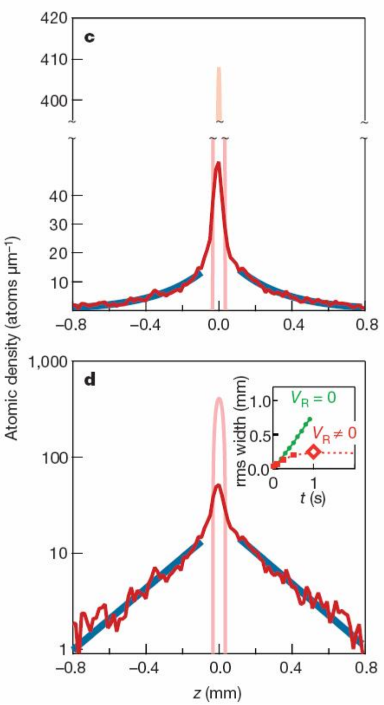


Experiments: propagation of light in disordered 1d waveguide lattices [Lahini et al., PRL (2008)]

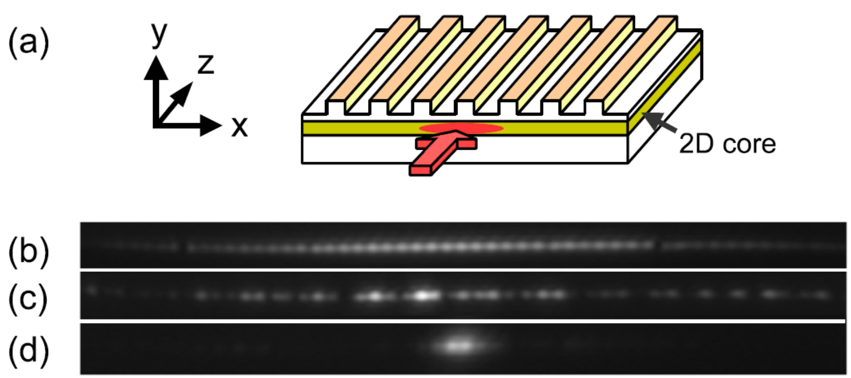

# The disordered Klein – Gordon (DKG) model

$$H_K = \sum_{l=1}^{N} \frac{p_l^2}{2} + \frac{\tilde{\varepsilon}_l}{2} u_l^2 + \frac{1}{4} u_l^4 + \frac{1}{2W}\left(u_{l+1} - u_l\right)^2$$

with **fixed boundary conditions** $u_0=p_0=u_{N+1}=p_{N+1}=0$. Typically N=1000.

**Parameters: W and the total energy E.** $\tilde{\varepsilon}_l$ **chosen uniformly from** $\left[\frac{1}{2},\frac{3}{2}\right]$.

**Linear case (neglecting the term $u_l^4/4$)**

**Ansatz: $u_l=A_l \exp(i\omega t)$. Normal modes (NMs) $A_{\nu,l}$ - Eigenvalue problem:**

$$\lambda A_l = \varepsilon_l A_l - (A_{l+1} + A_{l-1}) \text{ with } \lambda = W\omega^2 - W - 2, \quad \varepsilon_l = W(\tilde{\varepsilon}_l - 1)$$

# The disordered discrete nonlinear Schrödinger (DDNLS) equation

**We also consider the system:**

$$H_D = \sum_{l=1}^{N} \varepsilon_l \left|\psi_l\right|^2 + \frac{\beta}{2}\left|\psi_l\right|^4 - \left(\psi_{l+1}\psi_l^* + \psi_{l+1}^*\psi_l\right)$$

**where $\varepsilon_l$ chosen uniformly from $\left[-\frac{W}{2},\frac{W}{2}\right]$ and $\beta$ is the nonlinear parameter.**

**Conserved quantities: The energy and the norm $S=\sum_l \left|\psi_l\right|^2$ of the wave packet.**

# Distribution characterization

We consider normalized energy distributions $z_\nu \equiv \dfrac{E_\nu}{\sum_m E_m}$

with $E_\nu = \dfrac{p_\nu^2}{2} + \dfrac{\tilde{\varepsilon}_\nu}{2} u_\nu^2 + \dfrac{1}{4} u_\nu^4 + \dfrac{1}{4W}\left(u_{\nu+1} - u_\nu\right)^2$ for the DKG model,

and norm distributions $z_\nu \equiv \dfrac{\left|\psi_\nu\right|^2}{\sum_l \left|\psi_l\right|^2}$ for the DDNLS system.

**Second moment:** $m_2 = \sum_{\nu=1}^{N} \left(\nu - \bar{\nu}\right)^2 z_\nu$ with $\bar{\nu} = \sum_{\nu=1}^{N} \nu z_\nu$

**Participation number:** $P = \dfrac{1}{\sum_{\nu=1}^{N} z_\nu^2}$

measures the number of stronger excited modes in $z_\nu$.

Single site $P=1$. Equipartition of energy $P=N$.

# Different Dynamical Regimes

**Three expected evolution regimes** [Flach, Chem. Phys (2010) - S. & Flach, PRE (2010) - Laptyeva et al., EPL (2010) - Bodyfelt et al., PRE (2011)]

$\Delta$: width of the frequency spectrum, d: average spacing of interacting modes,

$\delta$: nonlinear frequency shift.

**Weak Chaos Regime: $\delta<d$, $m_2 \propto t^{1/3}$**

Frequency shift is less than the average spacing of interacting modes. NMs are weakly interacting with each other. [Molina, PRB (1998) – Pikovsky, & Shepelyansky, PRL (2008)].

**Intermediate Strong Chaos Regime: $d<\delta<\Delta$, $m_2 \propto t^{1/2} \longrightarrow m_2 \propto t^{1/3}$**

Almost all NMs in the packet are resonantly interacting. Wave packets initially spread faster and eventually enter the weak chaos regime.

**Selftrapping Regime: $\delta>\Delta$**

Frequency shift exceeds the spectrum width. Frequencies of excited NMs are tuned out of resonances with the nonexcited ones, leading to selftrapping, while a small part of the wave packet subdiffuses [Kopidakis et al., PRL (2008)].

# Single site excitations

**DDNLS W=4, β= 0.1, 1, 4.5  DKG W = 4, E = 0.05, 0.4, 1.5**

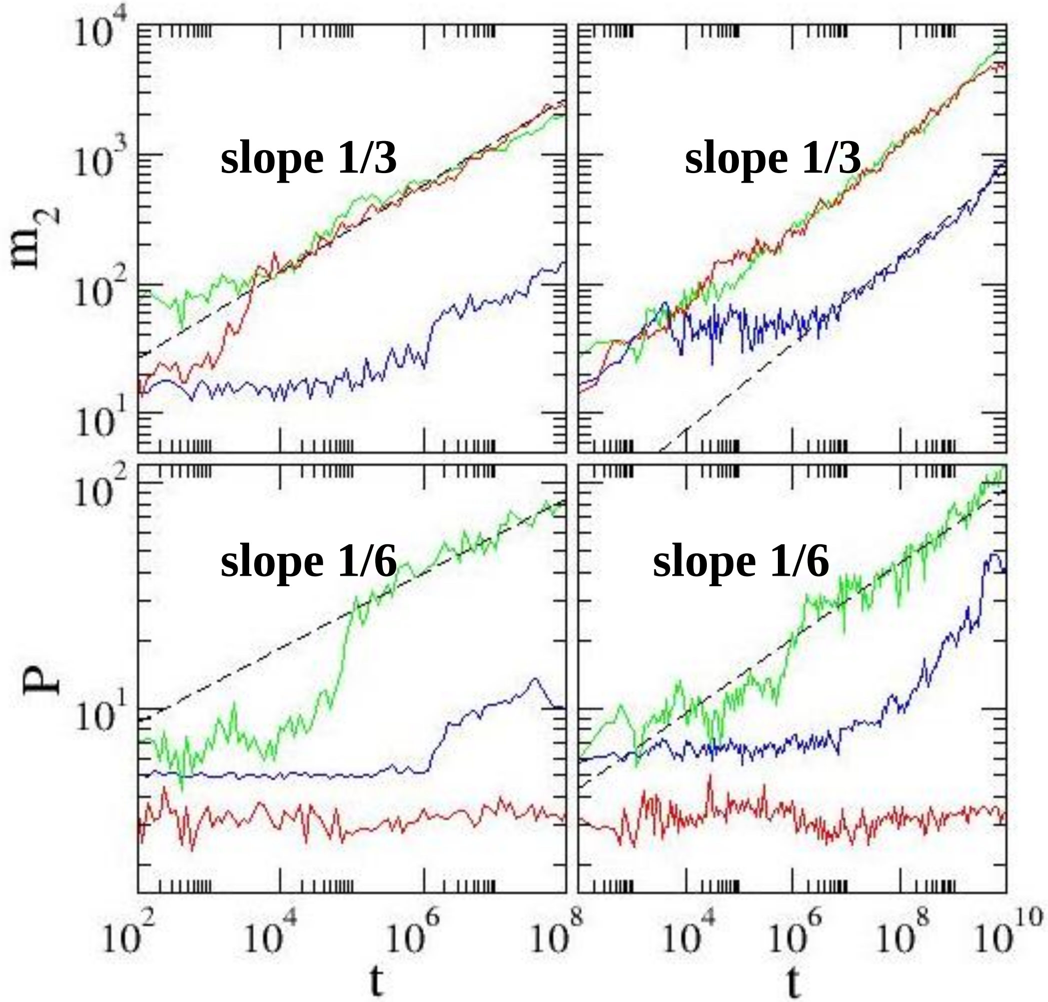


**No strong chaos regime**

**In weak chaos regime we averaged the measured exponent α ($m_2 \sim t^{\alpha}$) over 20 realizations:**

**α=0.33±0.05 (DKG)**

**α=0.33±0.02 (DDLNS)**

**Flach et al., PRL (2009)**

**S. et al., PRE (2009)**

# DKG: Different spreading regimes

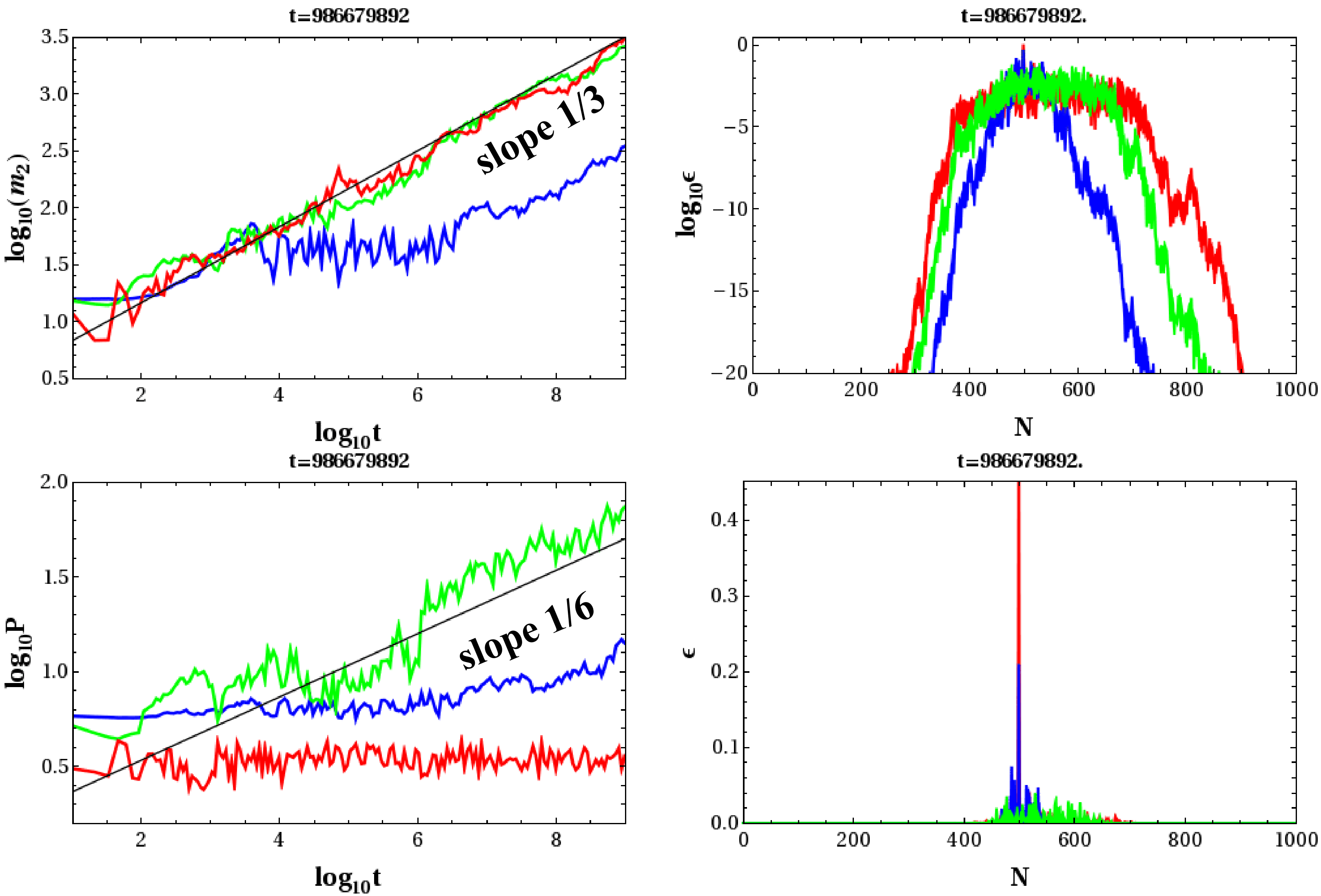

# Crossover from strong to weak chaos (block excitations)

DDNLS $\beta$= 0.04, 0.72, 3.6   DKG E= 0.01, 0.2, 0.75

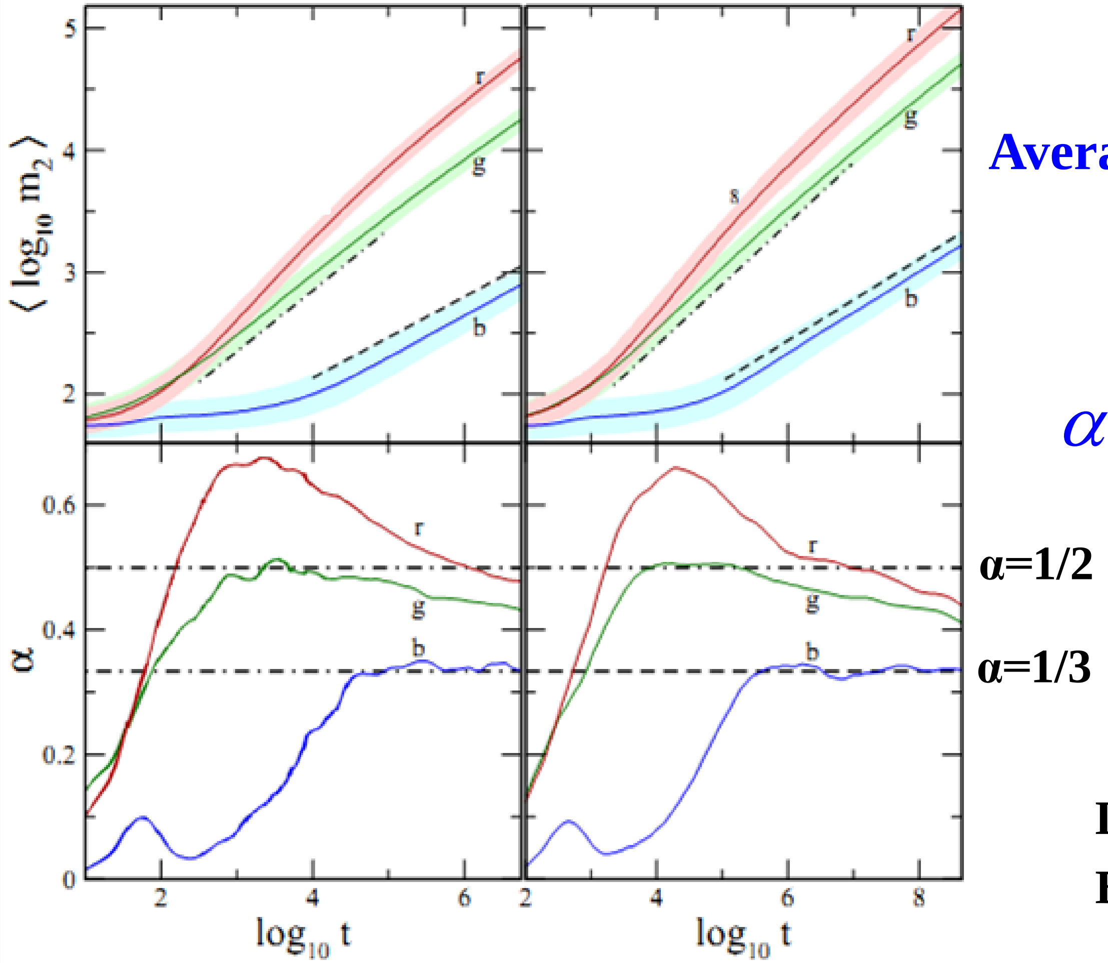


W=4

**Average over 1000 realizations!**

$$\alpha(\log t) = \frac{d\langle \log m_2 \rangle}{d \log t}$$

**Laptyeva et al., EPL (2010)**

**Bodyfelt et al., PRE (2011)**

# Variational Equations

**We use the notation $\mathbf{x} = (q_1,q_2,\ldots,q_N,p_1,p_2,\ldots,p_N)^T$. The deviation vector from a given orbit is denoted by**

$$\mathbf{v} = (\delta x_1, \delta x_2,\ldots,\delta x_n)^T \text{, with } n=2N$$

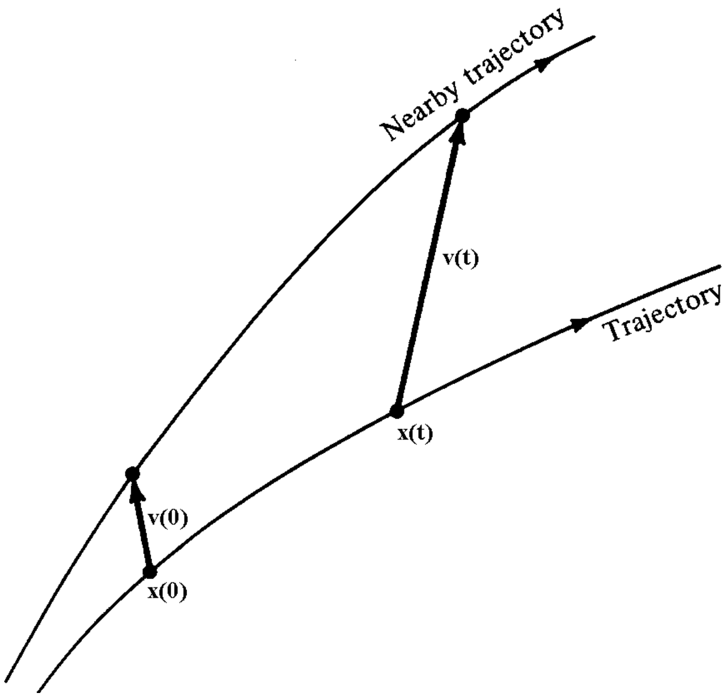


Benettin & Galgani, 1979, in Laval and Gressillon (eds.), op cit, 93

**The time evolution of v is given by the so-called variational equations:**

$$\frac{d\mathbf{v}}{dt} = -\mathbf{J} \cdot \mathbf{P} \cdot \mathbf{v}$$

**where**

$$\mathbf{J} = \begin{pmatrix} 0_N & -I_N \\ I_N & 0_N \end{pmatrix}, \quad P_{ij} = \frac{\partial^2 H}{\partial x_i \partial x_j} \quad i, j = 1, 2, \ldots, n$$

# Maximum Lyapunov Exponent

**Chaos: sensitive dependence on initial conditions.**

**Roughly speaking, the Lyapunov exponents of a given orbit characterize the mean exponential rate of divergence of trajectories surrounding it.**

**Consider an orbit in the 2N-dimensional phase space with initial condition x(0) and an initial deviation vector from it v(0). Then the mean exponential rate of divergence is:**

$$\mathrm{mLCE} = \lambda_1 = \lim_{t\to\infty} \Lambda(t) = \lim_{t\to\infty} \frac{1}{t} \ln \frac{\|v(t)\|}{\|v(0)\|}$$

$\lambda_1 = 0 \rightarrow$ **Regular motion**

$\lambda_1 \neq 0 \rightarrow$ **Chaotic motion**

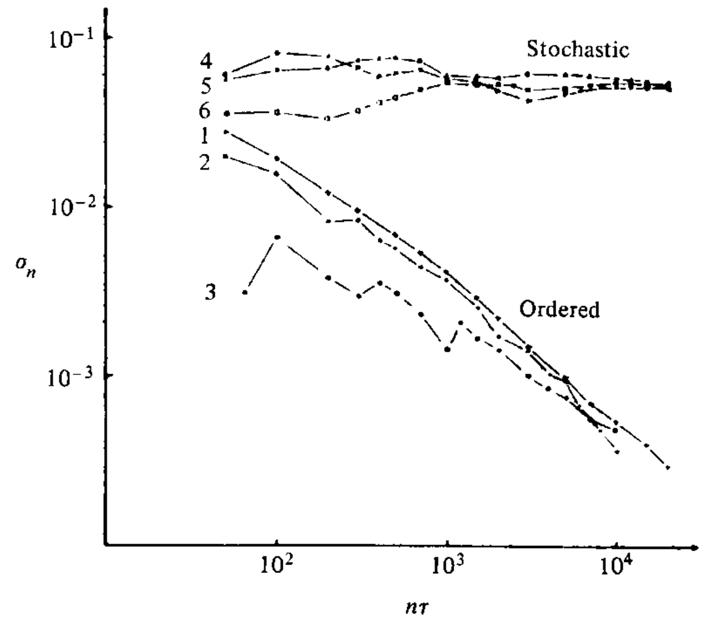


Figure 5.7. Behavior of $\sigma_n$ at the intermediate energy $E = 0.125$ for initial points taken in the ordered (curves 1–3) or stochastic (curves 4–6) regions (after Benettin *et al.*, 1976).

# Symplectic integration

We apply the 2-part splitting integrator ABA864 [Blanes et al., Appl. Num. Math. (2013) – Senyange & S., EPJ ST (2018)] to the DKG model:

$$H_K = \sum_{l=1}^{N}\left(\frac{p_l^2}{2} + \frac{\tilde{\varepsilon}_l}{2}u_l^2 + \frac{1}{4}u_l^4 + \frac{1}{2W}\left(u_{l+1} - u_l\right)^2\right)$$

and the 3-part splitting integrator $ABC^6_{[SS]}$ [S. et al., Phys. Let. A (2014) – Gerlach et al., EPJ ST (2016) – Danieli et al., MinE (2019)] to the DDNLS system:

$$H_D = \sum_l \varepsilon_l \left|\psi_l\right|^2 + \frac{\beta}{2}\left|\psi_l\right|^4 - \left(\psi_{l+1}\psi_l^* + \psi_{l+1}^*\psi_l\right), \qquad \psi_l = \frac{1}{\sqrt{2}}\left(q_l + ip_l\right)$$

$$H_D = \sum_l \left(\frac{\varepsilon_l}{2}\left(q_l^2 + p_l^2\right) + \frac{\beta}{8}\left(q_l^2 + p_l^2\right)^2 - q_n q_{n+1} - p_n p_{n+1}\right)$$

By using the so-called Tangent Map method we extend these symplectic integration schemes in order to integrate simultaneously the variational equations [S. & Gerlach, PRE (2010) – Gerlach & S., Discr. Cont. Dyn. Sys. (2011) – Gerlach et al., IJBC (2012)].

# DKG: Weak Chaos

**Block excitation**
**L=37 sites,**
**E=0.37, W=3**

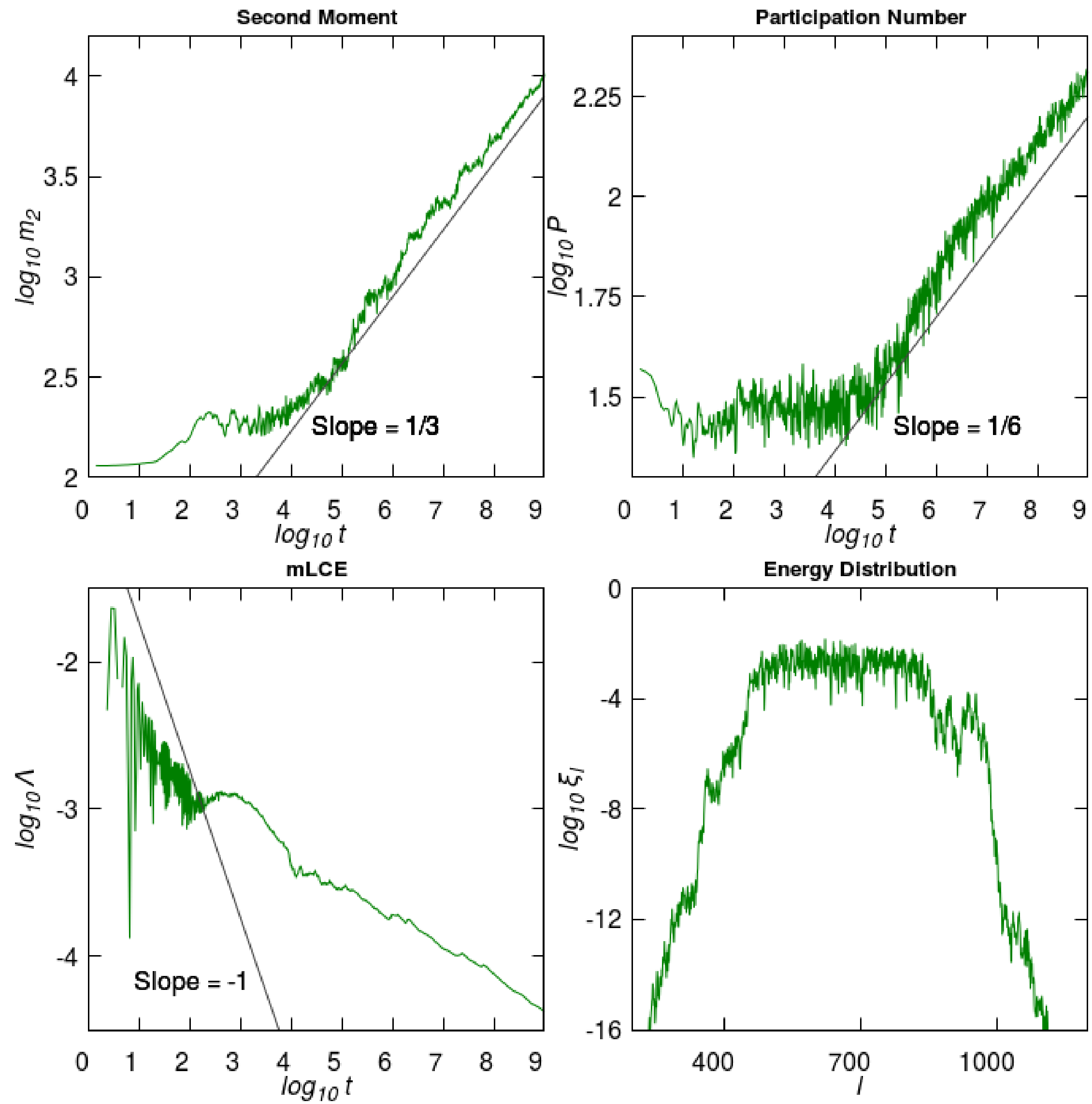

# DKG: Weak Chaos

**Individual runs**
**Linear case**
**E=0.4, W=4**

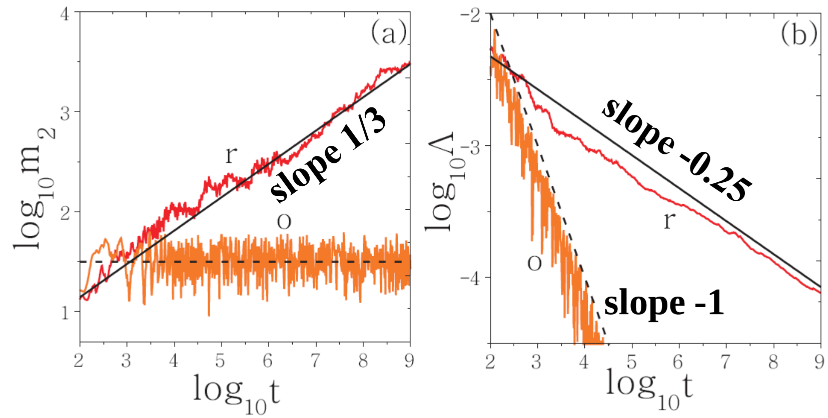


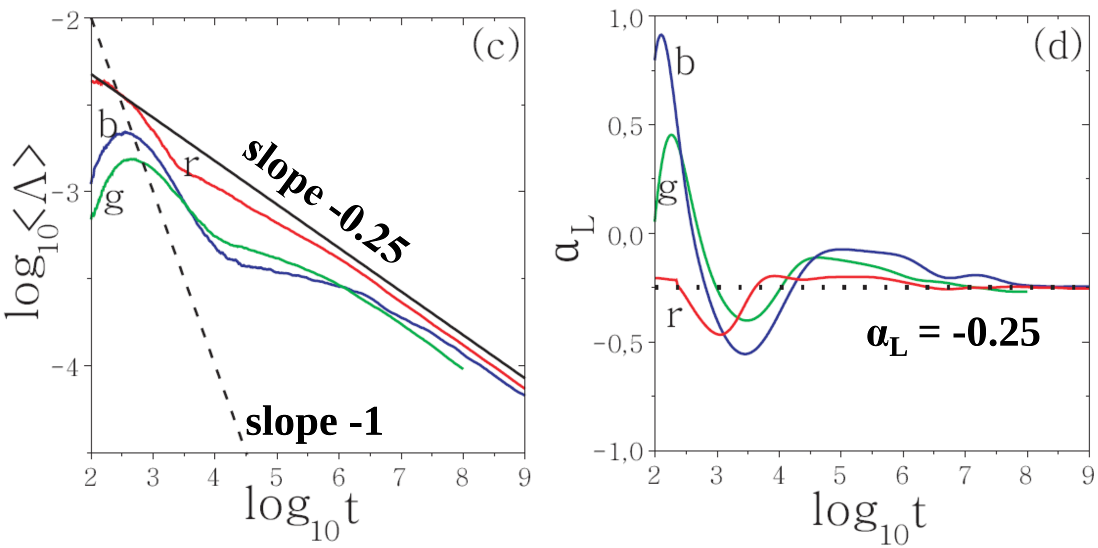


$$\alpha_L = \frac{d\left(\log\langle\Lambda\rangle\right)}{d\log t}$$

**Average over 50 realizations**

**Single site excitation E=0.4, W=4**
**Block excitation (L=21 sites) E=0.21, W=4**
**Block excitation (L=37 sites) E=0.37, W=3**

**S. et al., PRL (2013)**

# Weak Chaos: DKG and DDNLS

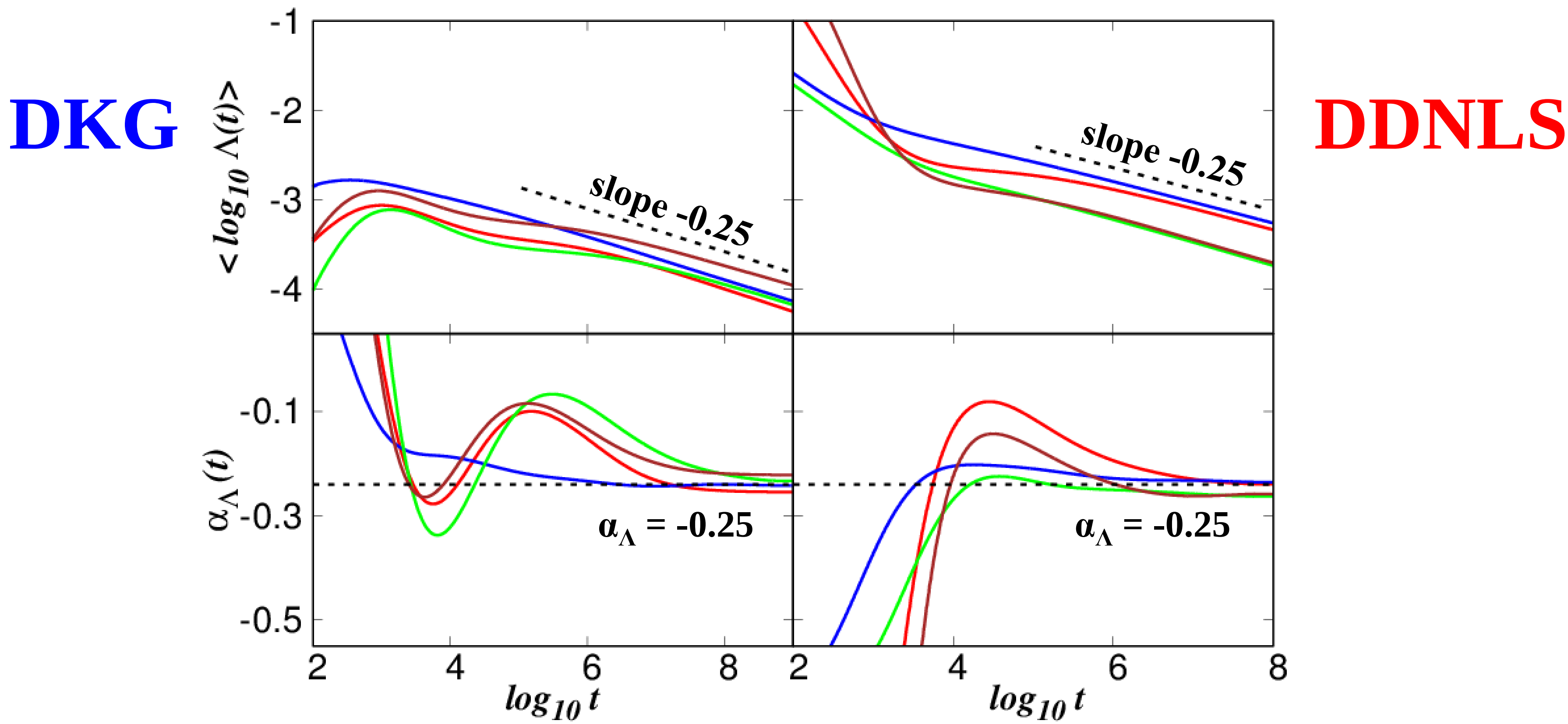


**Average over 100 realizations [Senyange, Many Manda & S., PRE (2018)]**

| DKG | DDNLS |
|---|---|
| **Block excitation (L=37 sites) E=0.37, W=3** | **Block excitation (L=21 sites) β=0.04, W=4** |
| **Single site excitation E=0.4, W=4** | **Single site excitation β=1, W=4** |
| **Block excitation (L=21 sites) E=0.21, W=4** | **Single site excitation β=0.6, W=3** |
| **Block excitation (L=13 sites) E=0.26, W=5** | **Block excitation (L=21 sites) β=0.03, W=3** |

# Strong Chaos: DKG and DDNLS

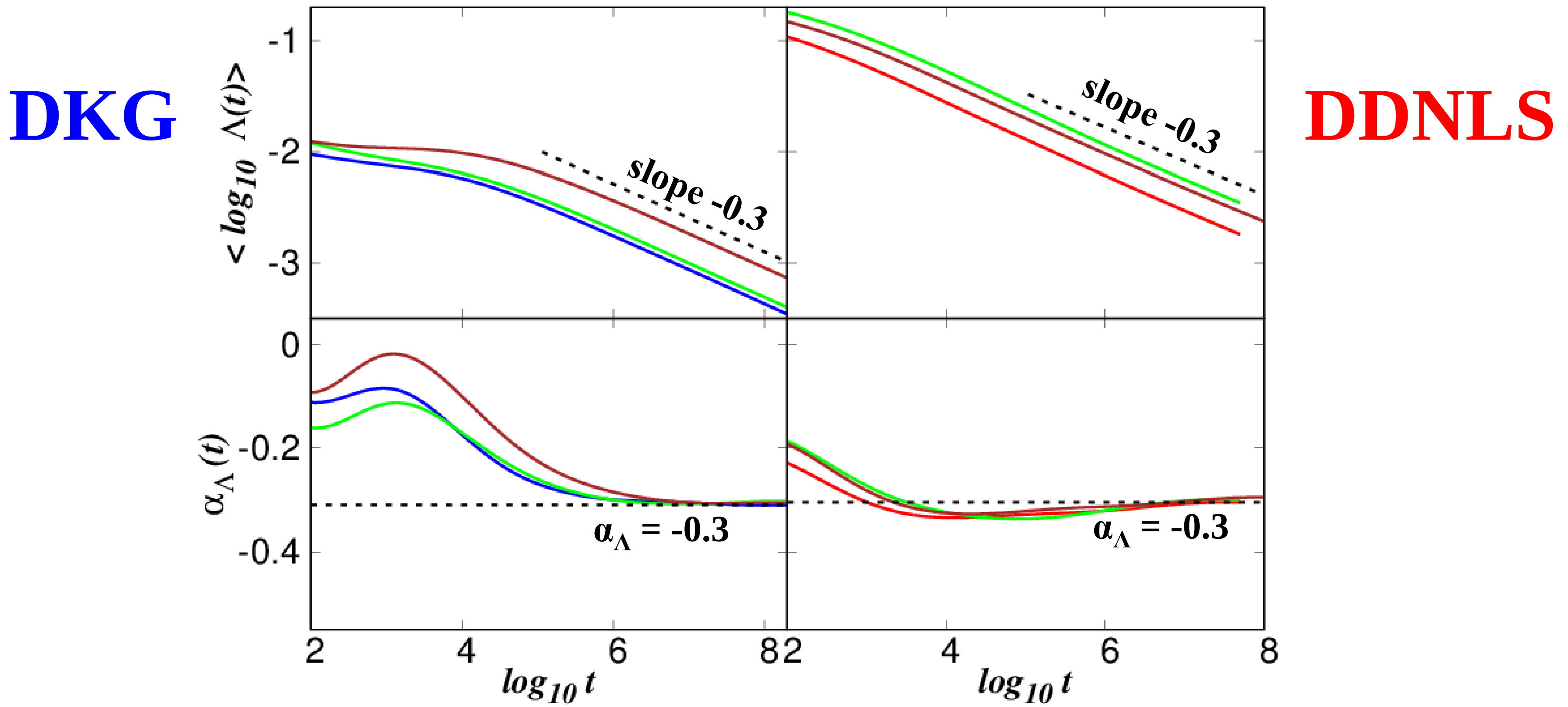


**Average over 100 realizations [Senyange, Many Manda & S., PRE (2018)]**

**Block excitation (L=83 sites) E=0.83, W=2**
**Block excitation (L=37 sites) E=0.37, W=3**
**Block excitation (L=83 sites) E=0.83, W=3**

**Block excitation (L=21 sites) β=0.62, W=3.5**
**Block excitation (L=21 sites) β=0.5, W=3**
**Block excitation (L=21 sites) β=0.72, W=3.5**

# Deviation Vector Distributions (DVDs)

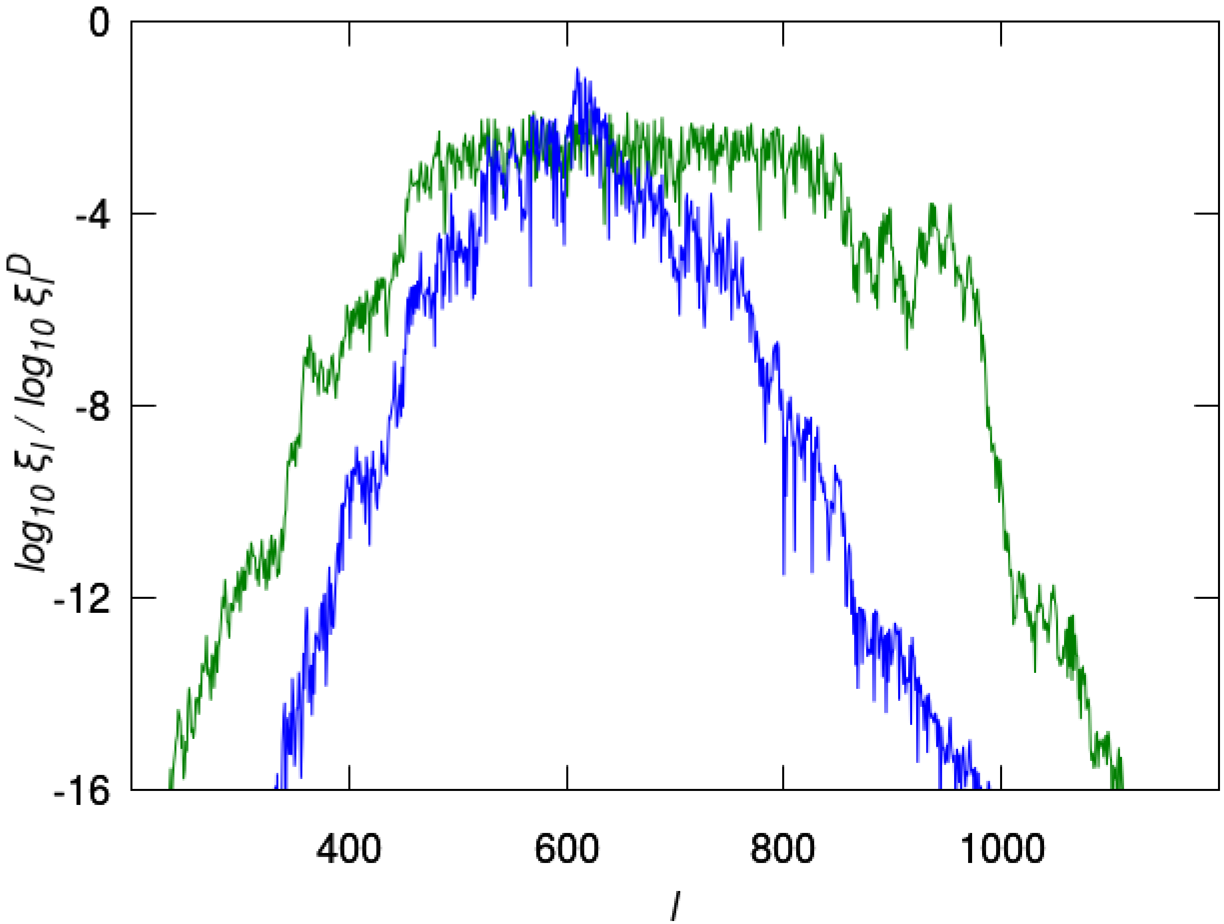


**Energy**
**DVD**

**DKG**
**weak chaos**
**L=37 sites,**
**E=0.37, W=3**

**Deviation vector:**
**$v(t)=(\delta u_1(t), \delta u_2(t),\ldots, \delta u_N(t), \delta p_1(t), \delta p_2(t),\ldots, \delta p_N(t))$**

$$\textbf{DVD:}\ \xi_l^D = \frac{\delta u_l^2 + \delta p_l^2}{\sum_l \left(\delta u_l^2 + \delta p_l^2\right)}$$

# Deviation Vector Distributions (DVDs)

**DKG: weak chaos. L=37 sites, E=0.37, W=3**

**Energy**

**DVD**

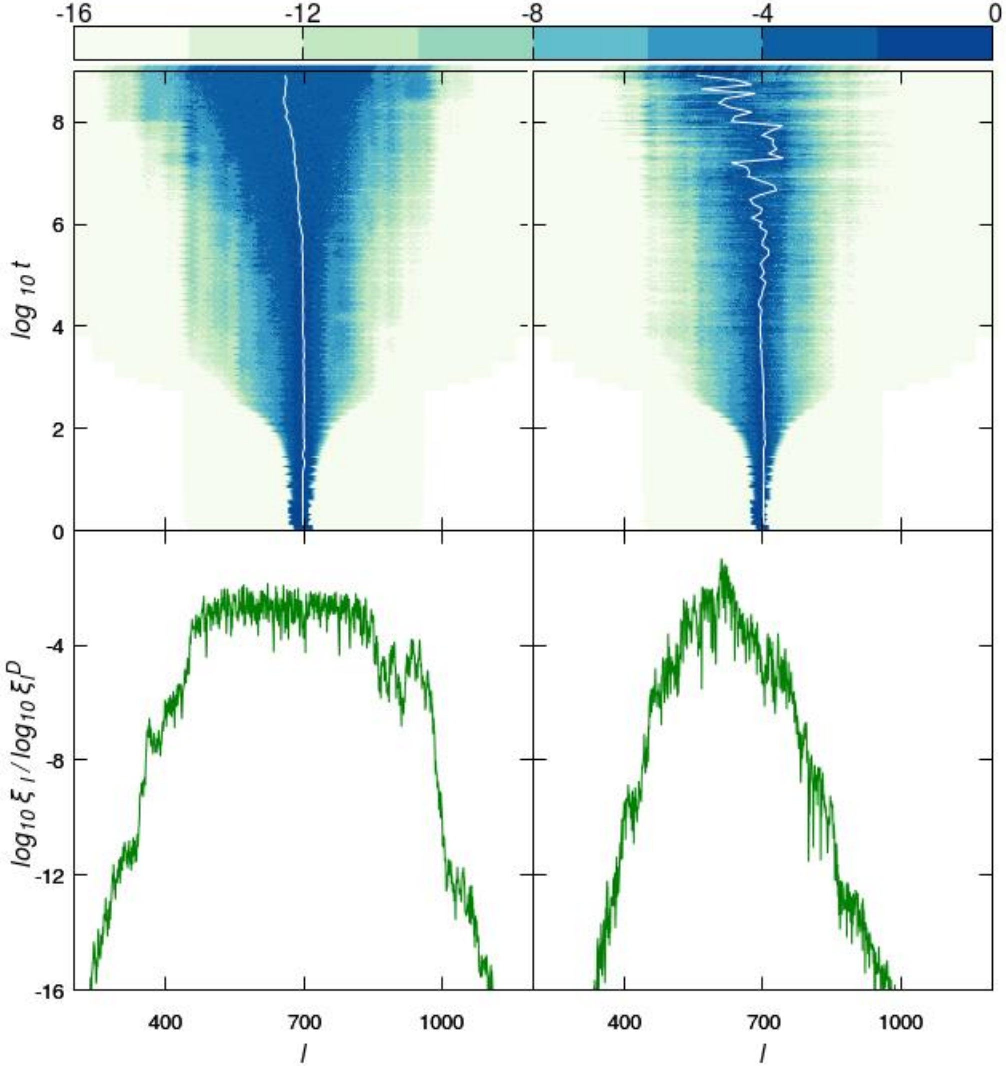

# Weak Chaos: DKG and DDNLS

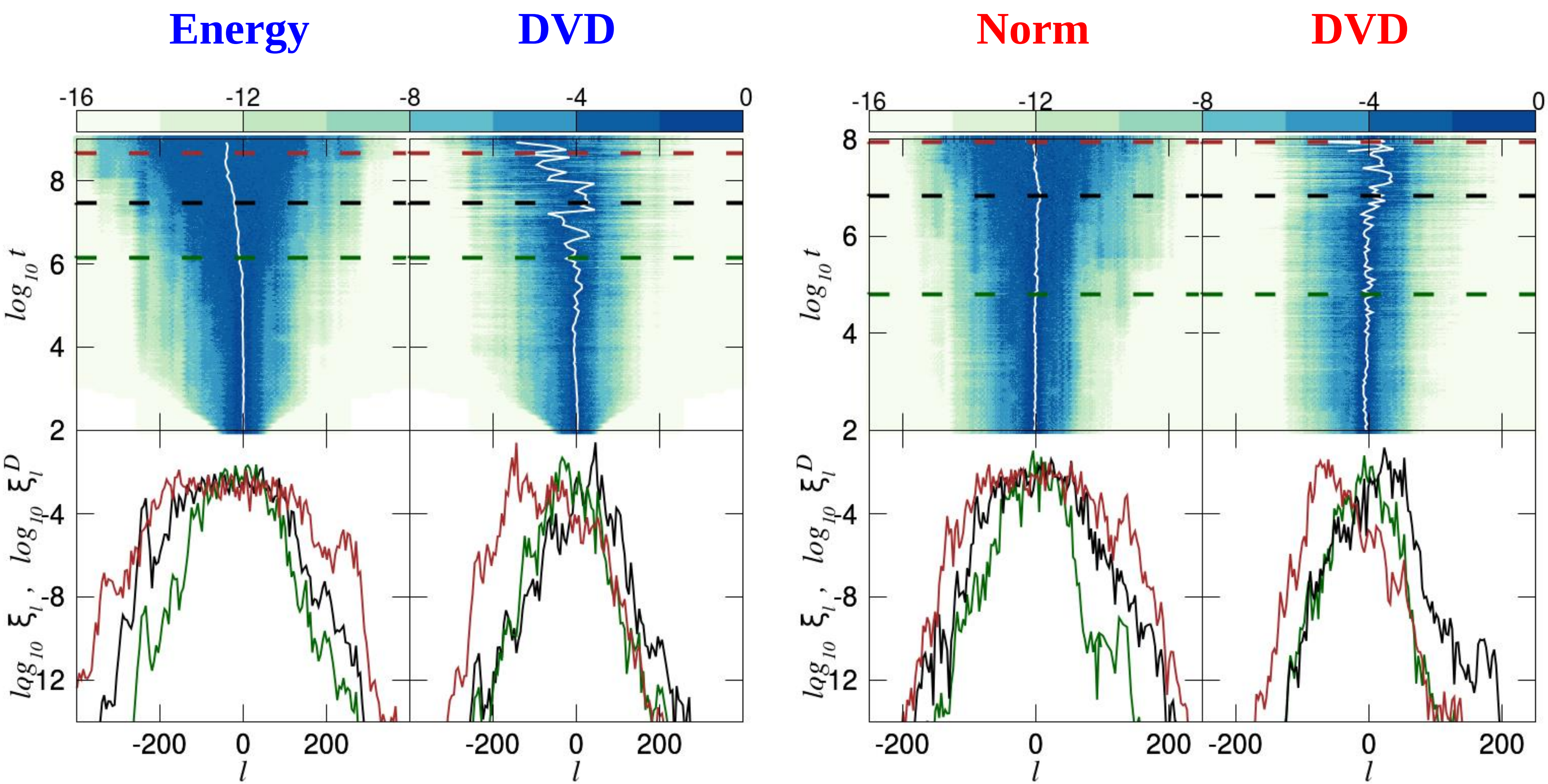


**DKG: W=3, L=37, E=0.37**

**DDNLS: W=4, L=21, β=0.04**

# Deviation Vector Distributions (DVDs)

**DDNLS: strong chaos W=3.5, L=21, β=0.72**

**Norm**

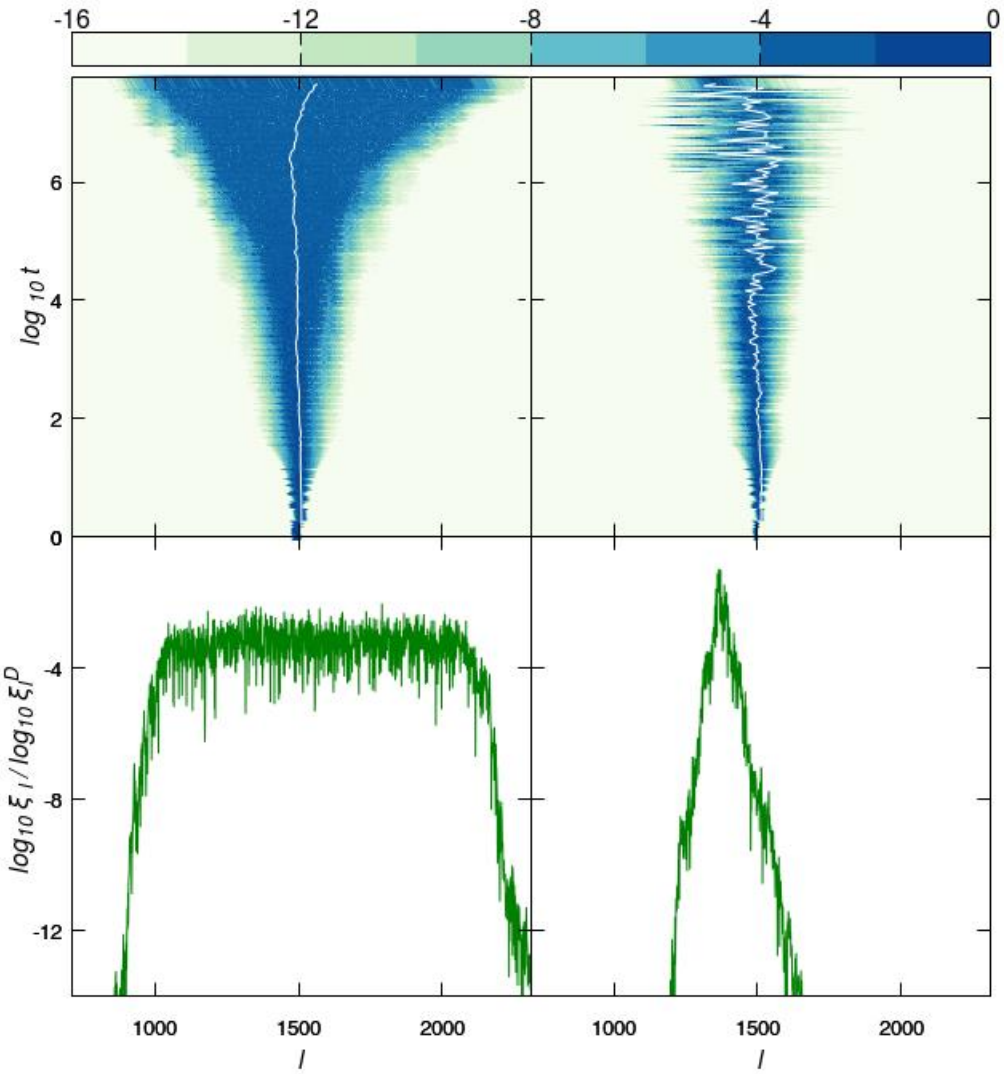


**DVD**

# Strong Chaos: DKG and DDNLS

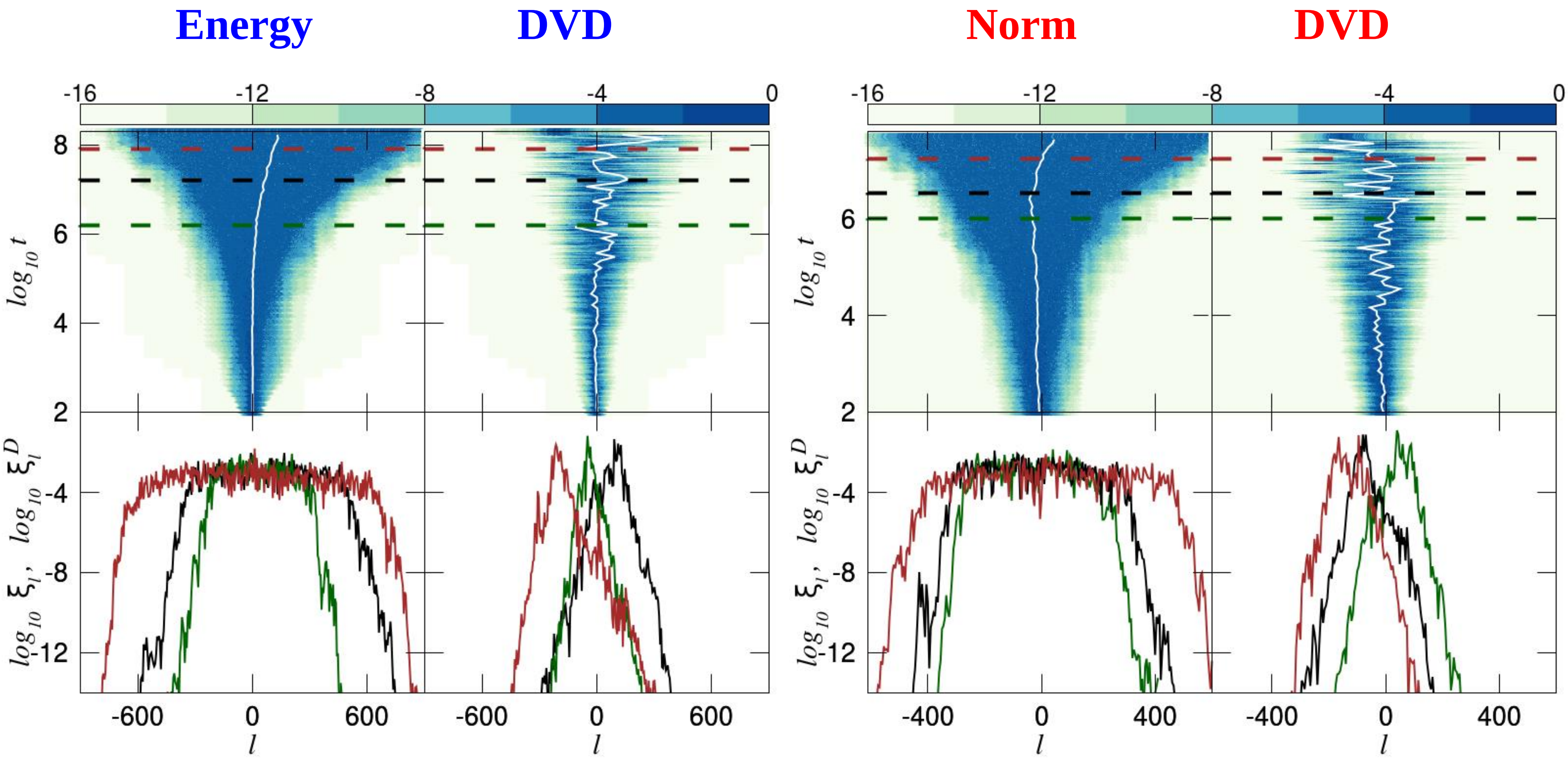


DKG: W=3, L=83, E=8.3

DDNLS: W=3.5, L=21, β=0.72

# Characteristics of DVDs

## Weak chaos

## Strong chaos

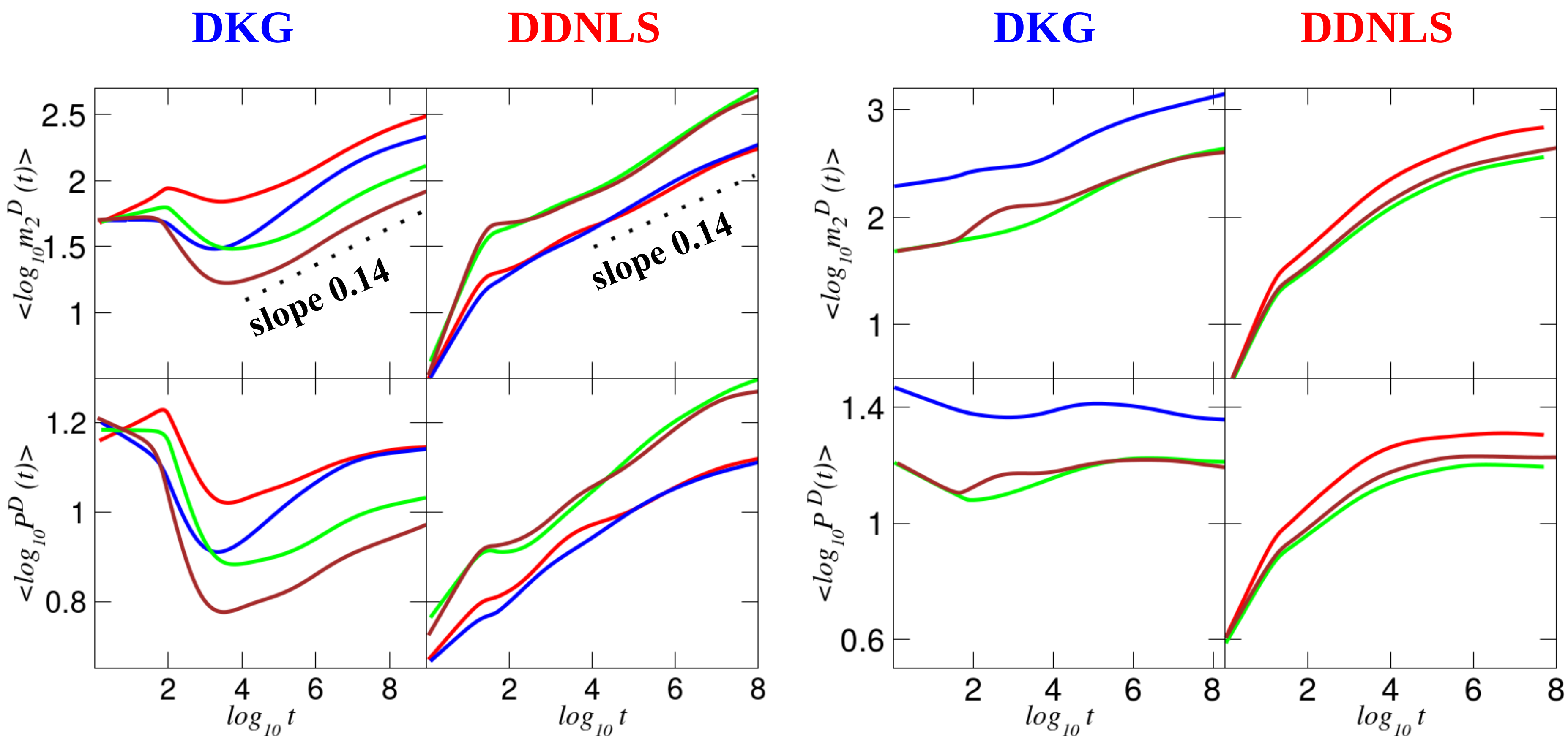

# Characteristics of DVDs

**KG weak chaos**
**L=37, E=0.37, W=3**

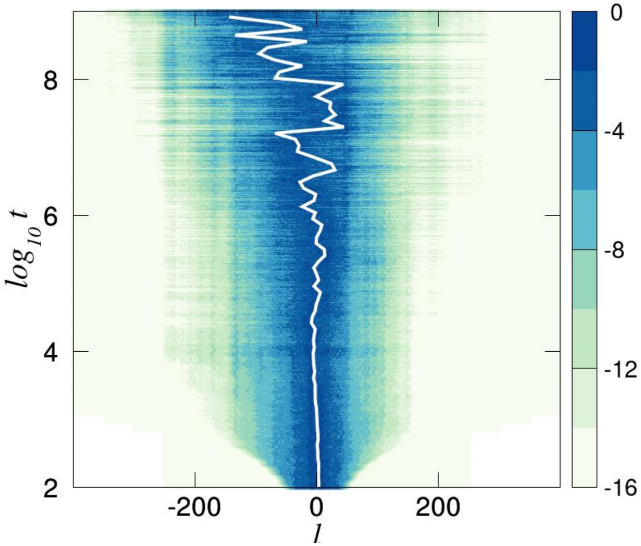


**Range of the lattice visited by the DVD**

$$R(t) = \max_{[0,t]}\left\{\overline{l}_w(t)\right\} - \min_{[0,t]}\left\{\overline{l}_w(t)\right\}$$

$$\overline{l}_w = \sum_{l=1}^{N} l \xi_l^D$$

**DKG** **DDNLS**

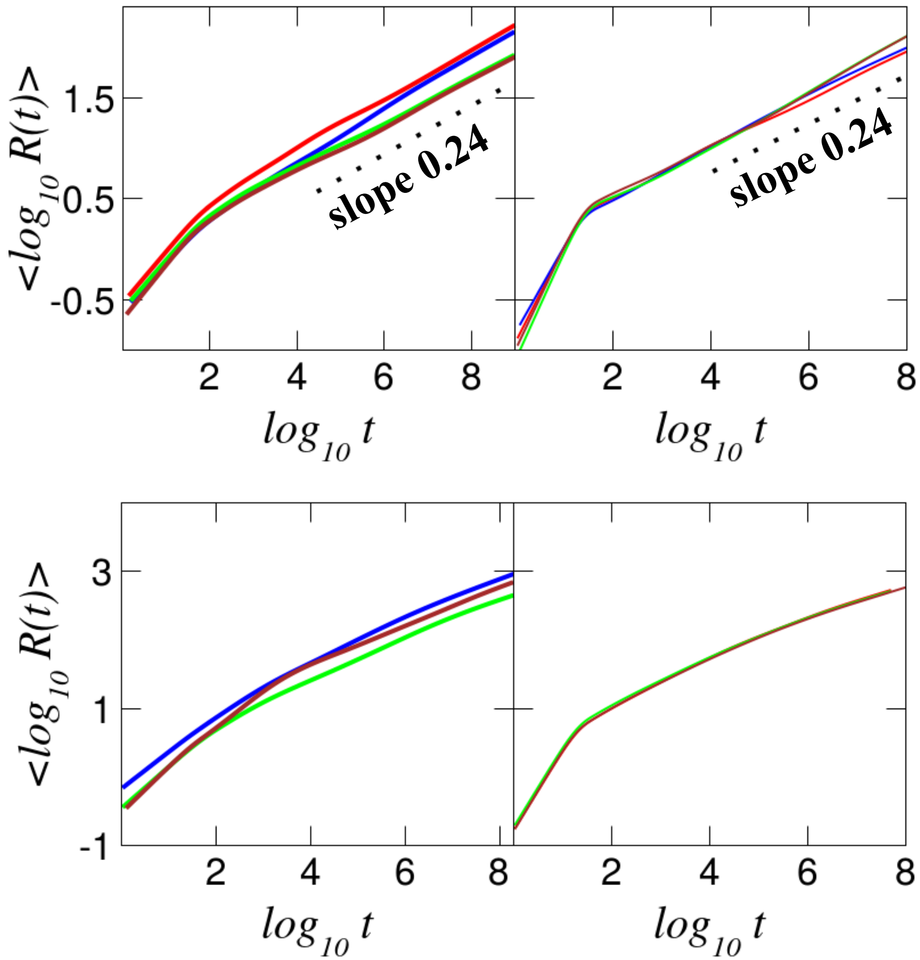


**Weak chaos**

**Strong chaos**

# Granular chains

# Work in collaboration with

Vassos Achilleos (Université du Maine, France)

Arnold Ngapasare (PhD student, Université du Maine, France)

Olivier Richoux (Université du Maine, France)

Georgios Theocharis (Université du Maine, France)

# Granular media

**Examples: coal, sand, rice, nuts, coffee etc.**

**1D granular chain (experimental control of nonlinearity and disorder)**

# Hamiltonian model

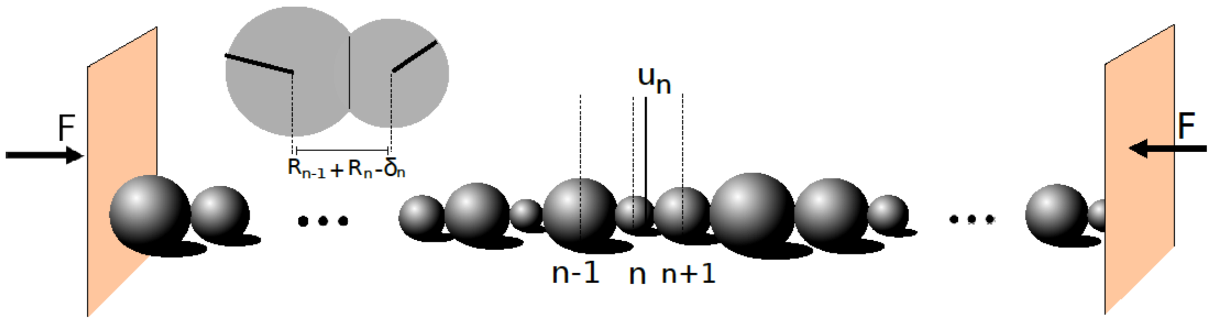


$$H=\sum_{n=1}^{N}\left(\frac{p_n^2}{2m_n}+\frac{2}{5}A_n[\delta_n+u_{n-1}-u_n]_+^{5/2}-\frac{2}{5}A_n\delta_n^{5/2}-A_n\delta_n^{3/2}(u_{n-1}-u_n)\right)$$

$$\delta_n=(F/A_n)^{2/3} \qquad A_n=(2/3)\mathcal{E}\sqrt{(R_{n-1}R_n)/(R_{n-1}+R_n)}/(1-\nu^2)$$

**$[x]_+$=0 if x<0: formation of a gap (non-smooth nonlinearities).**

**Hertzian forces between spherical beads. $\nu$: Poisson's ratio, $\mathcal{E}$: Elastic modulus.**

# Hamiltonian model

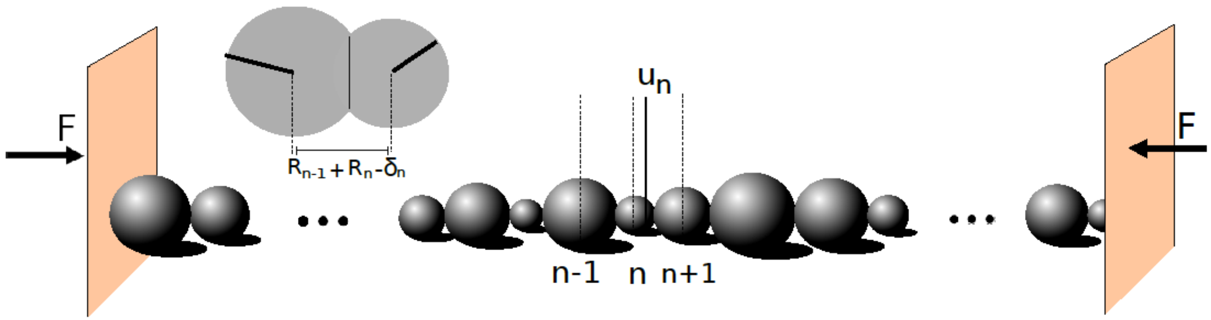


$$H=\sum_{n=1}^{N}\left(\frac{p_n^2}{2m_n}+\frac{2}{5}A_n[\delta_n+u_{n-1}-u_n]_+^{5/2}-\frac{2}{5}A_n\delta_n^{5/2}-A_n\delta_n^{3/2}(u_{n-1}-u_n)\right)$$

$$\delta_n=(F/A_n)^{2/3} \qquad A_n=(2/3)\mathcal{E}\sqrt{(R_{n-1}R_n)/(R_{n-1}+R_n)}/(1-\nu^2)$$

**$[x]_+$=0 if x<0: formation of a gap (non-smooth nonlinearities).**

**Hertzian forces between spherical beads. $\nu$: Poisson's ratio, $\mathcal{E}$: Elastic modulus.**

**Disorder both in couplings and masses**
**$R_n \in [R, \alpha R]$ with $\alpha \geq 1$**

**Mean radius = 0.01 m, $\alpha$=5 , F=1N, Fixed boundary conditions**

# Eigenmodes and single site excitations

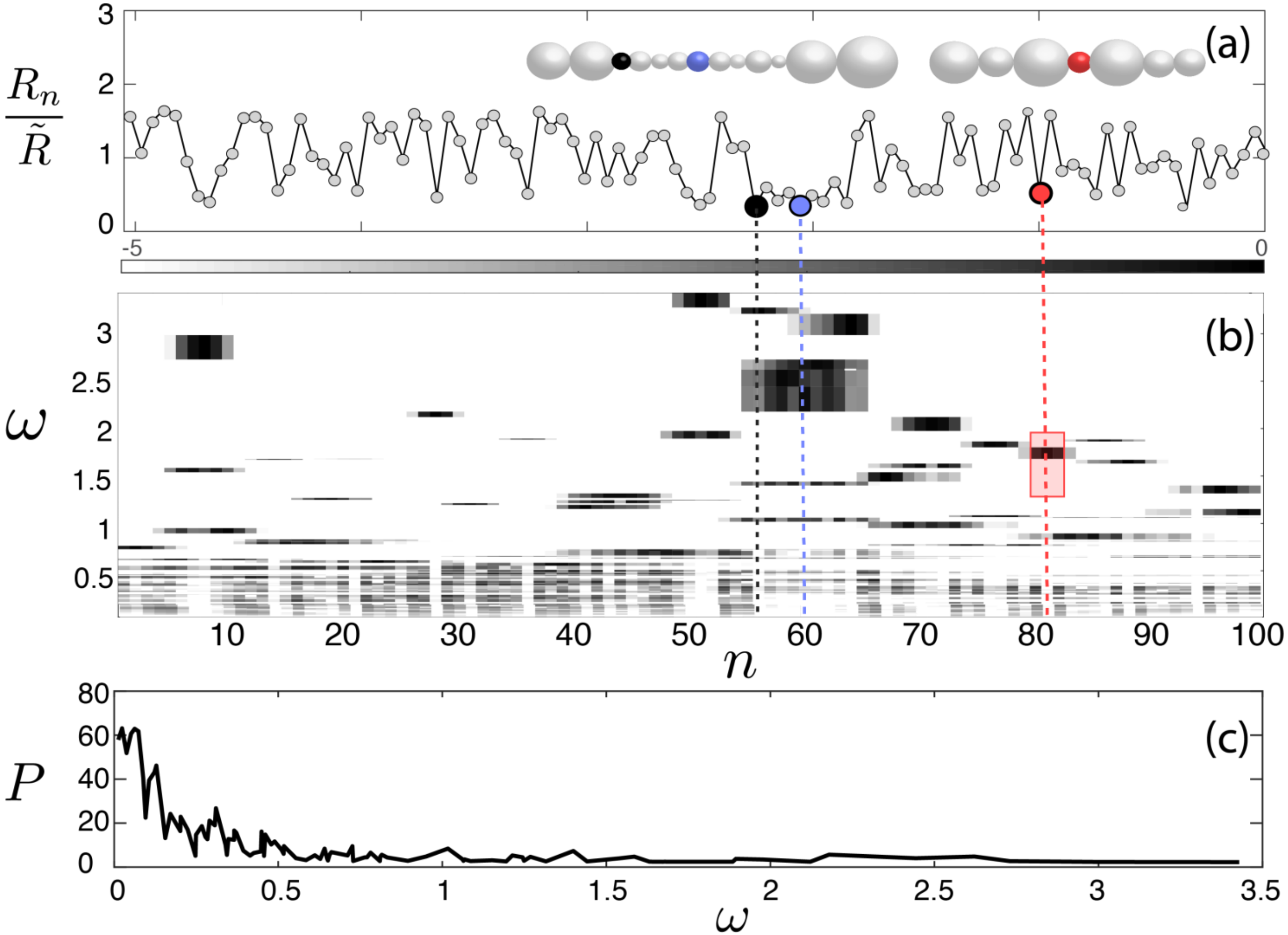


**Disorder realization with N=100 beads**

**Displacement excitation of bead n**

**Participation number of eigenmodes. About 10 extended modes with P>40**

**Achilleos et al., PRE, 2018**

# Weak nonlinearity: Long time evolution

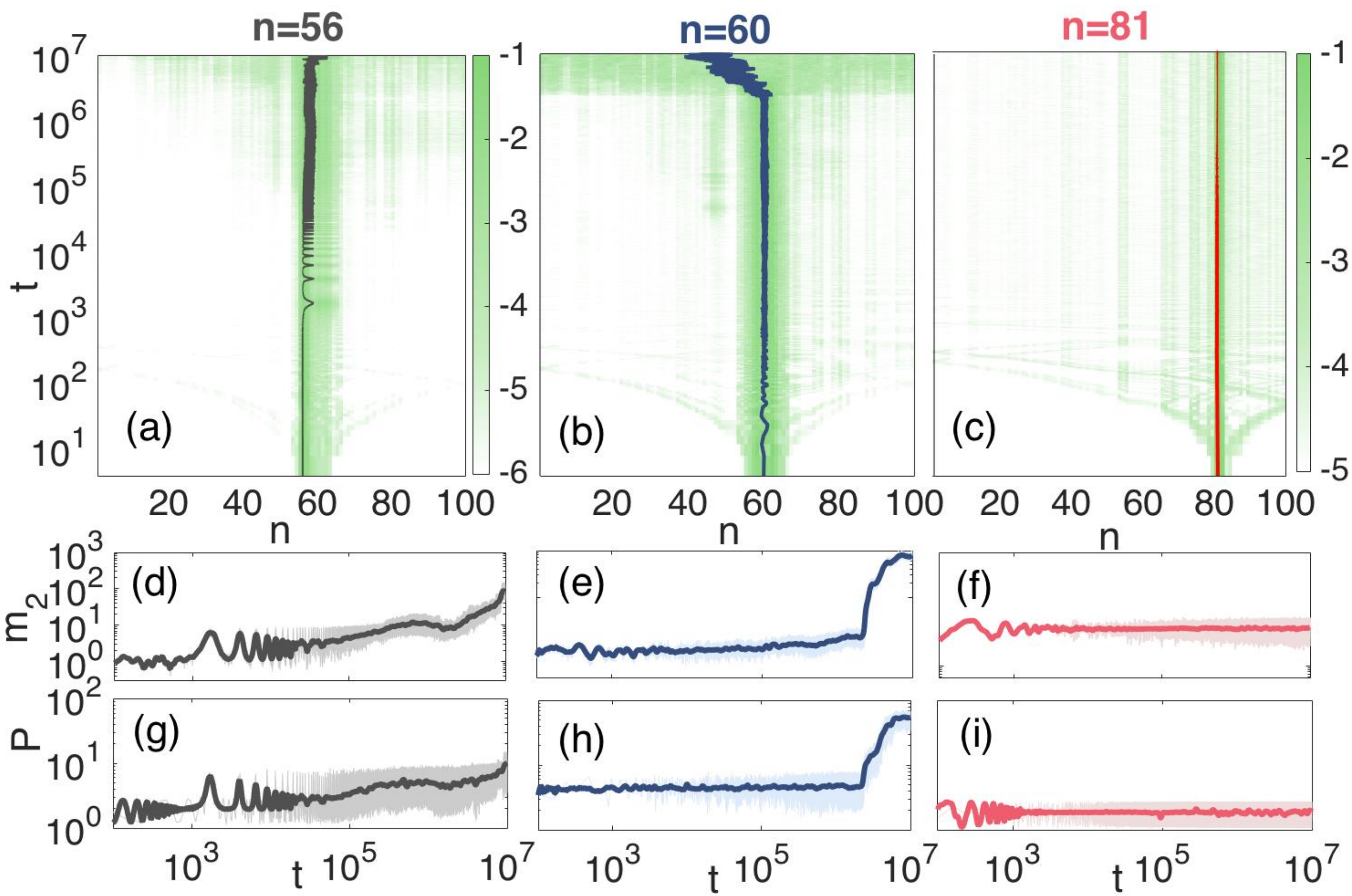


**Delocalization** **Delocalization** **Localization**

# Weak nonlinearity: Chaoticity

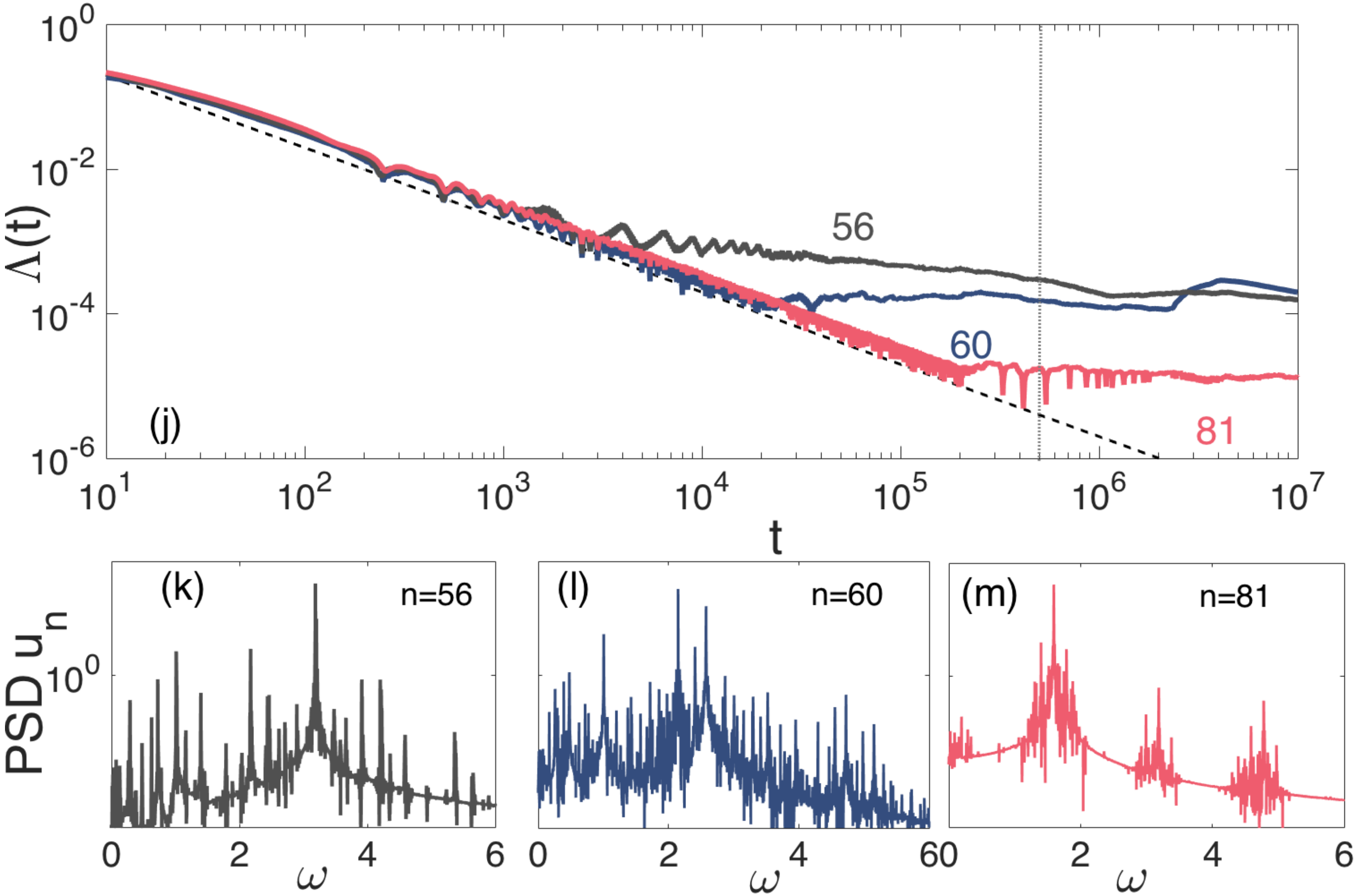


mLCE

Power Spectrum Distribution

Weakly chaotic motion: Delocalization

Long-lived chaotic Anderson-like Localization

# Strong nonlinearity: Equipartition

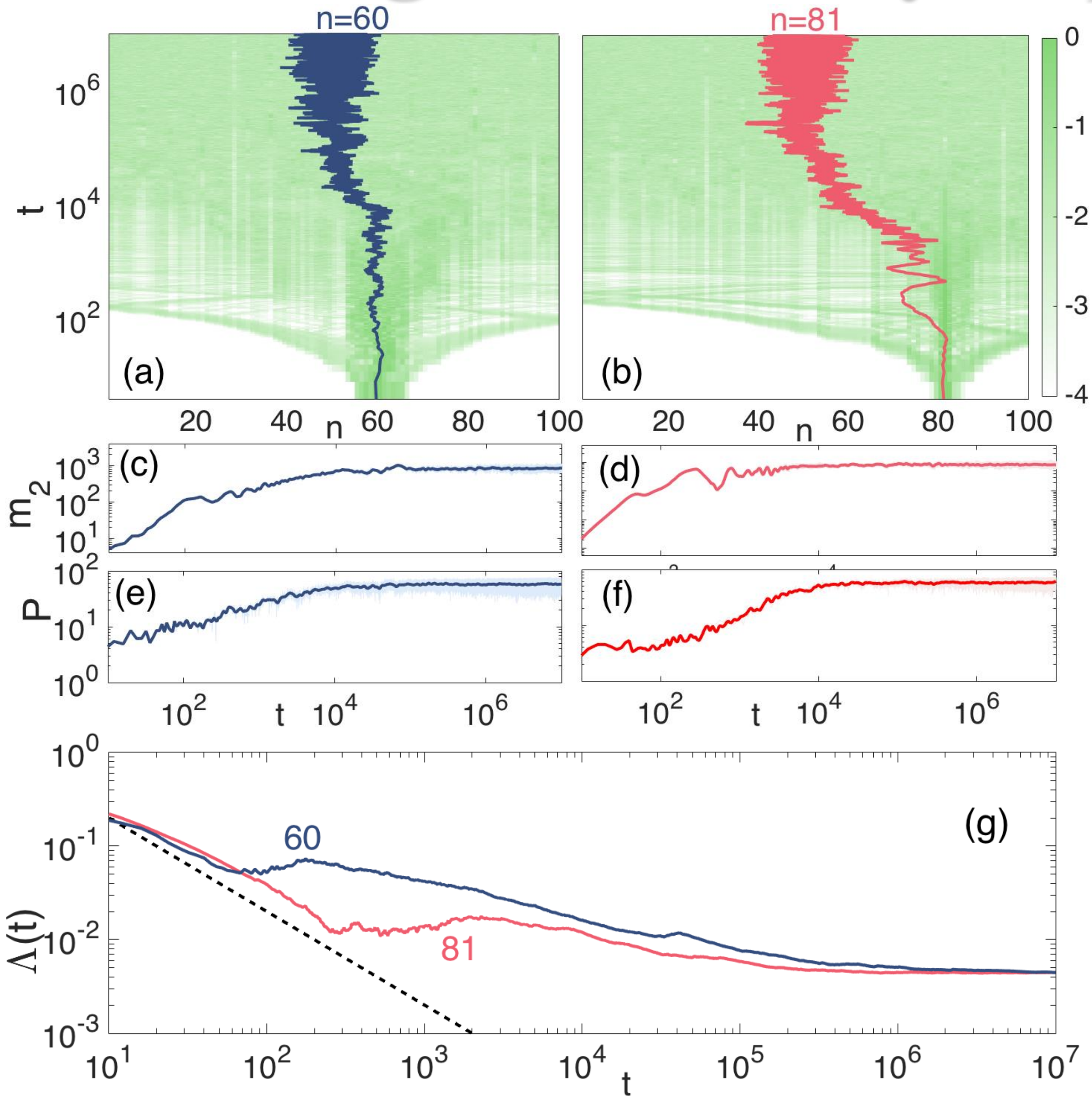


**The granular chain reaches energy equipartition and an equilibrium chaotic state, independent of the initial position excitation.**

# Comparison with the FPUT model

**Hertzian model $H_H$:**

$$H_H = \sum_{n=1}^{N}\left[\frac{p_n^2}{2m_n} + \frac{2}{5}A_n\left[\delta_n + u_{n+1} - u_n\right]_+^{5/2} - \frac{2}{5}A_n\delta_n^{5/2} - A_n\delta_n^{3/2}\left(u_{n-1} - u_n\right)\right]$$

**Using**

**a) Taylor series expansion up to fourth order and**

**b) assuming small displacements, i.e. $u_n/\delta_{n,n+1} \ll 1$**

**we obtain the disordered α+β FPUT model $H_F$:**

$$H_F = \sum_{n=1}^{N}\left[\frac{p_n^2}{2m_n} + K_n^{(2)}\left(u_n - u_{n-1}\right)^2 + K_n^{(3)}\left(u_n - u_{n-1}\right)^3 + K_n^{(4)}\left(u_n - u_{n-1}\right)^4\right]$$

**with**

$$K_n^{(2)} = \frac{3}{2}A_n\delta_n^{1/2}, \quad K_n^{(3)} = -\frac{3}{8}A_n\delta_n^{-1/2}, \quad K_n^{(4)} = \frac{3}{48}A_n\delta_n^{-3/2}$$

# Dynamical evolution of an initially localized mode

**We consider a particular strongly disordered chain of N=40 particles with α=5 (Ngapasare et al., PRE, 2019).**

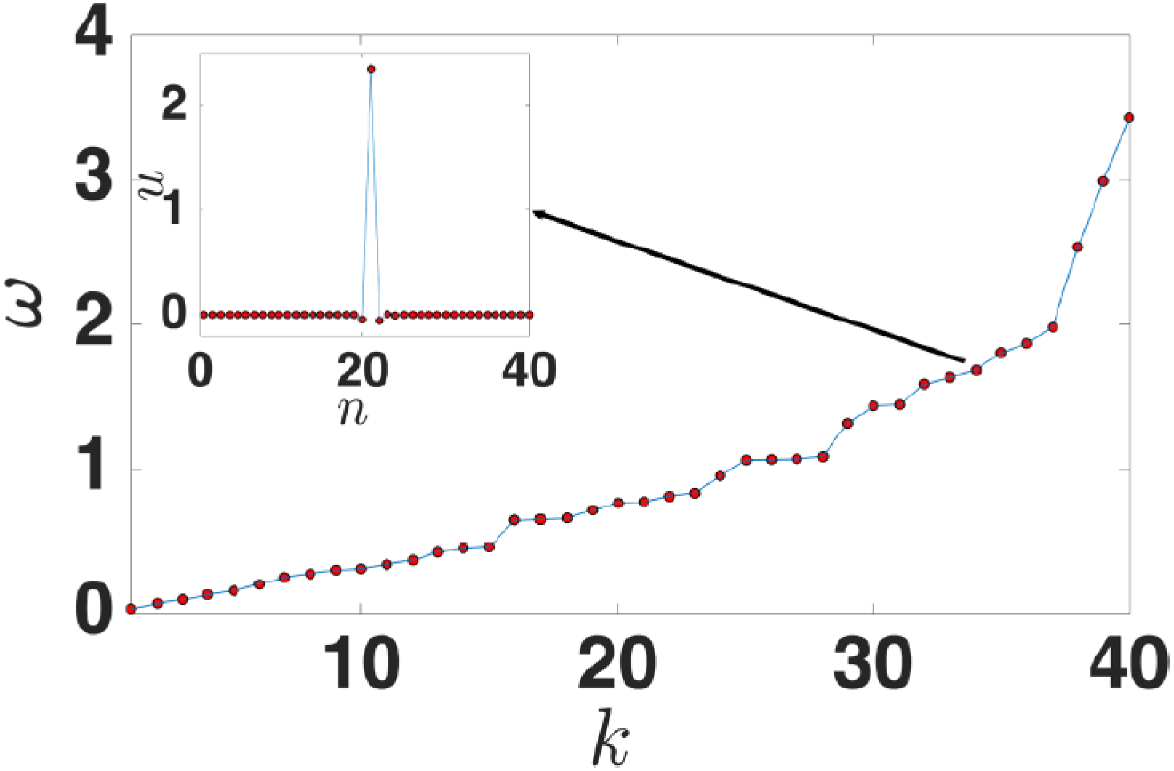


**Mode k=34 is strongly localized at site n=21.**

# Entropy and equipartition

**Weighted harmonic energies ($E_k$ is the kth mode's energy):** $v_k = E_k / \sum_{k=1}^{N} E_k$

**Spectral entropy:** $S(t) = -\sum_{k=1}^{N} v_k(t) \ln v_k(t)$ **with** $0 < S \leq S_{max} = \ln N$

**Normalized spectral entropy:** $\eta(t) = \dfrac{S(t) - S_{max}}{S(0) - S_{max}}$

**Dynamics close to initially excited modes:**

$$\eta \approx 1$$

**Equipartition [Goedde et al., Phys. D (1992) – Danieli et al., PRE (2017)]:**

$$\eta(t) \to \langle \eta \rangle = \frac{1 - C}{\ln N - S(0)}, \quad C \approx 0.5772$$

# Weak nonlinearity: Near linear limit

Energy distribution

Herzian

FPUT

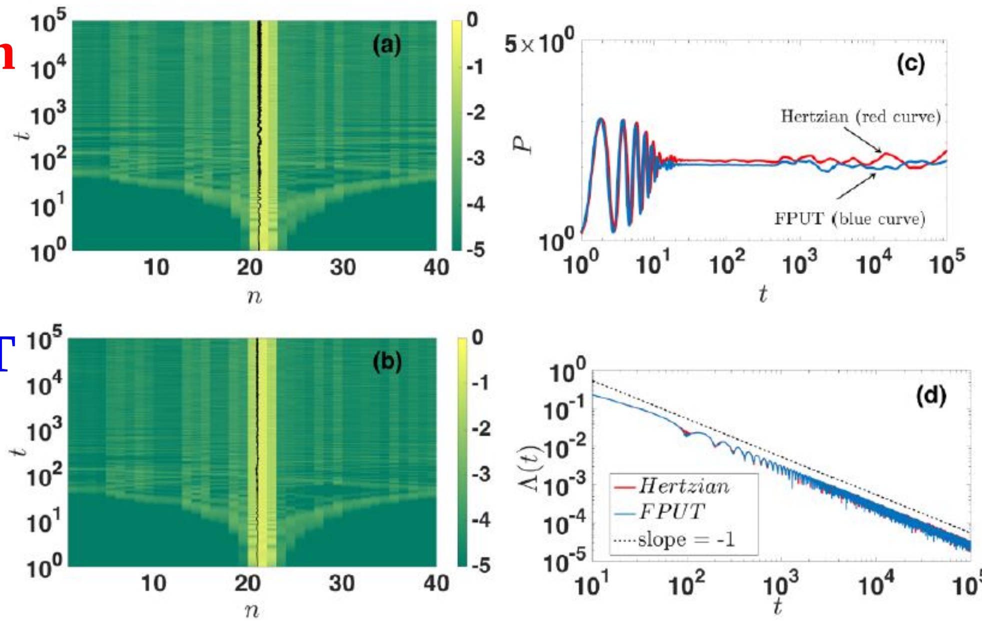


DVD

Herzian

FPUT

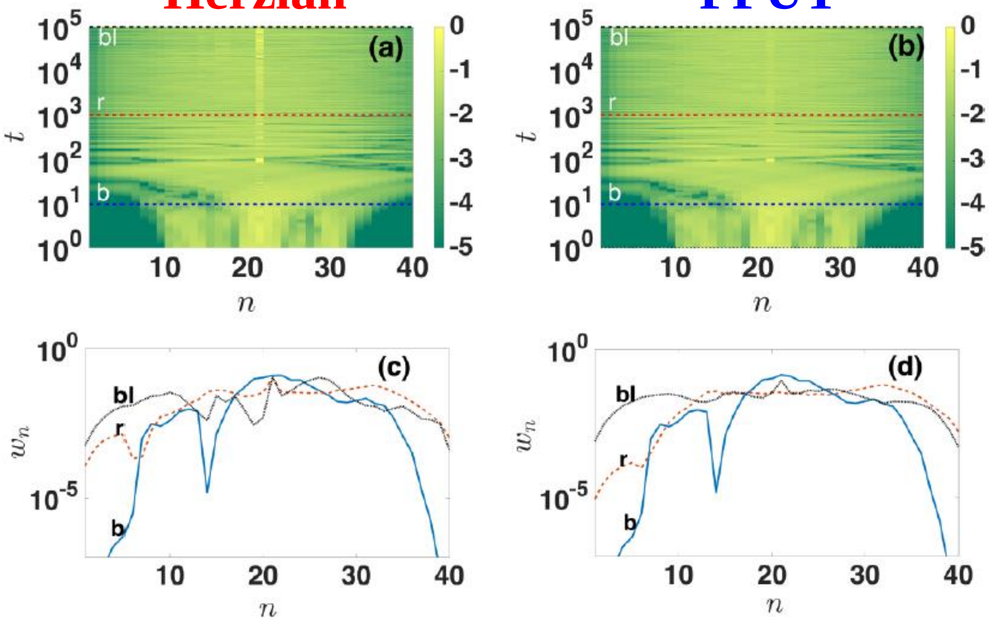


**Single site (n=21) excitation for small energies (H=0.25):**

**Both models behave the same.**
**Localization without chaos.**
**DVDs are extended.**

# Hertzian model: Route to equipartition

**H=0.5**

**Energy distribution**

**H=1.8**

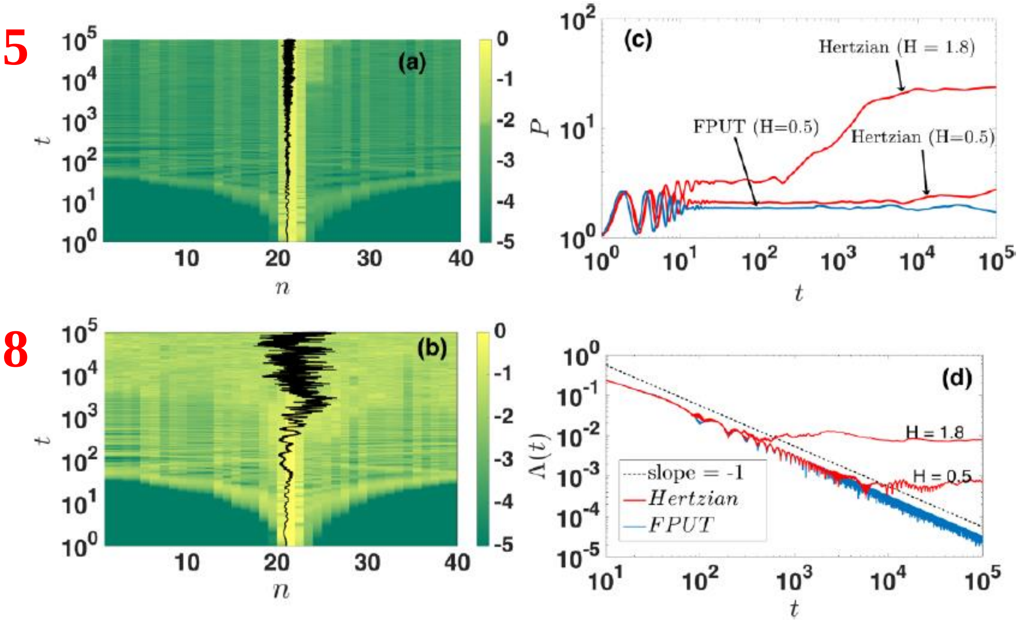


**DVD**

**H=0.5** **H=1.8**

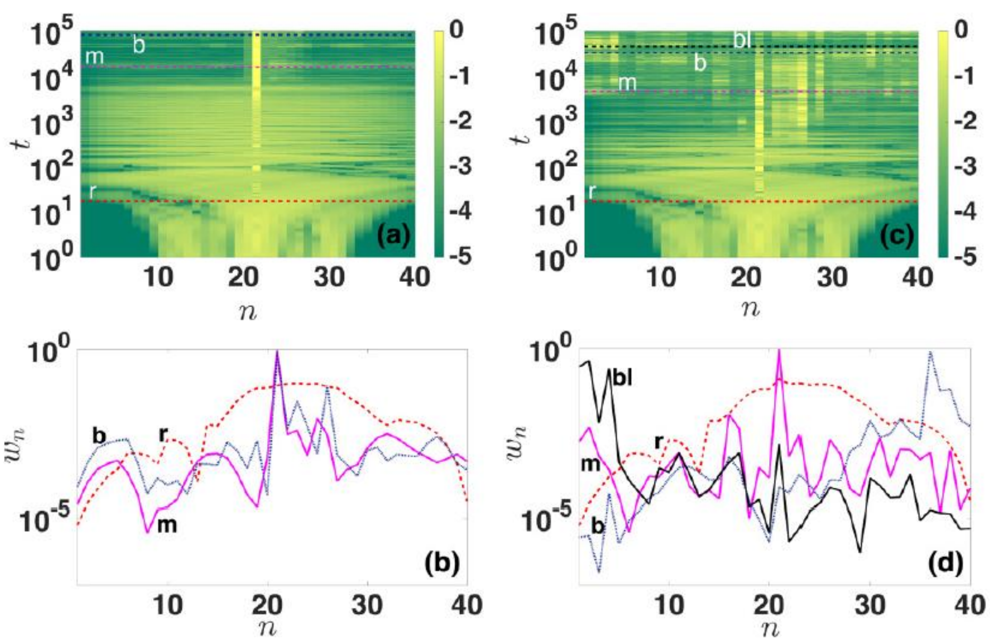


**As energy increases the Herzian system exhibits:**
**localized chaos (e.g. H=0.5) and eventually extended chaos above a threshold value (H≳1.8).**
**DVDs become localized.**

**FPUT: localized and regular up to H=1.8.**

# Hertzian model: Route to equipartition

**Gaps:** the main ingredient which introduces (even localized) chaos

**Spreading of gaps:** related to the introduction of extended chaos

H=0.5 H=1.8

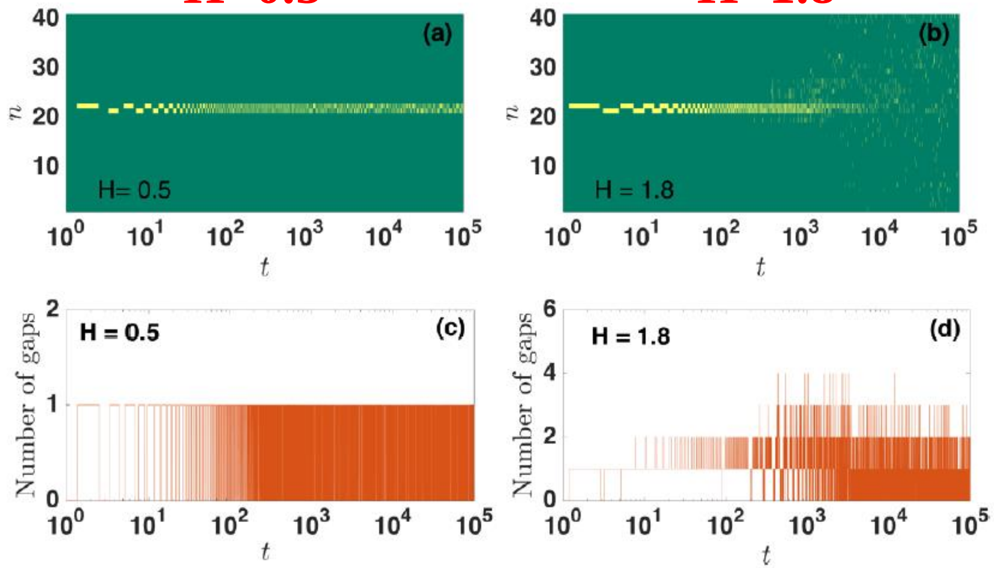


## Normalized spectral entropy

H=0.25 H=0.5 H=1.8 H=3

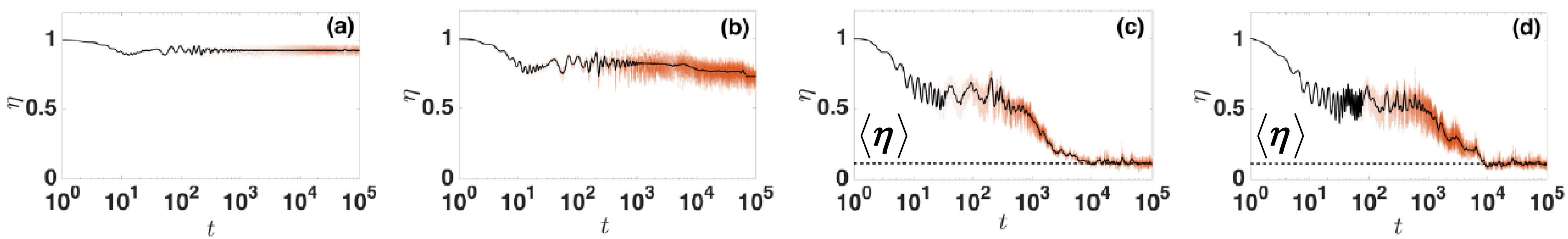

# FPUT model: Alternate behavior

**Energy increase** **does not necessarily lead to delocalization,** **despite the fact that the system is chaotic.**

**Energy** **DVD**

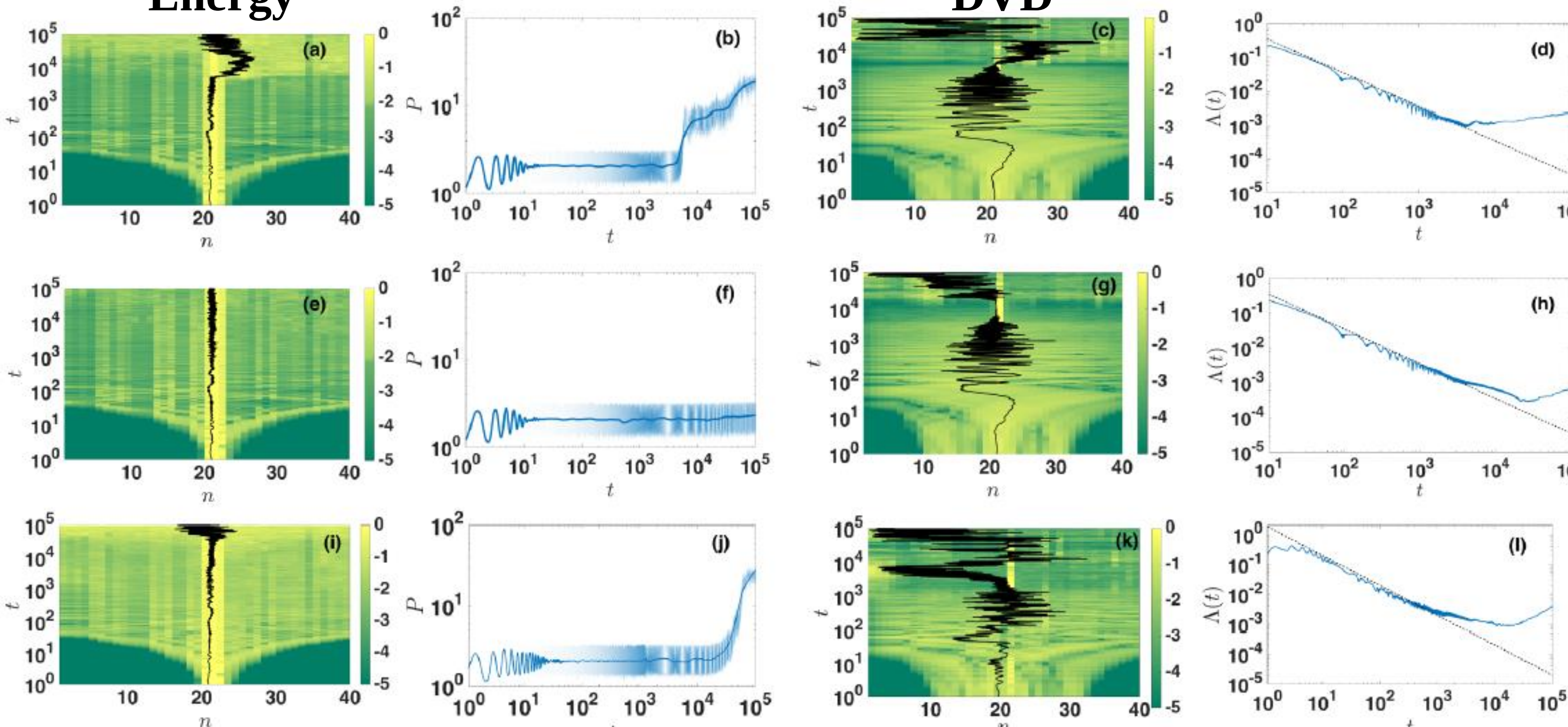


**H=2.9**

**H=4**

**H=8.7381**

**Normalized spectral entropy**

**H=0.25** **H=2.9** **H=4** **H=8.7381**

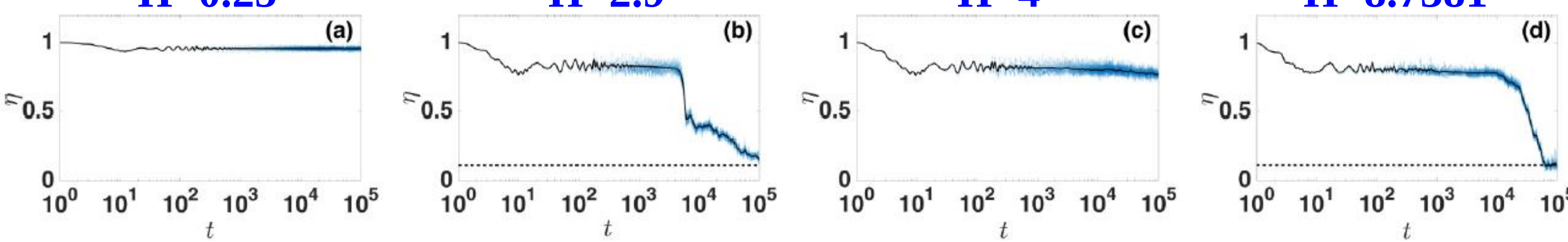

# The

# PBD model of DNA

# Work in collaboration with

Malcolm Hillebrand (PhD student)

George Kalosakas (University of Patras, Greece)

# DNA structure

**Double helix with two types of bonds:**

- **Adenine-thymine (AT) – two hydrogen bonds**
- **Guanine-cytosine (GC) – three hydrogen bonds**

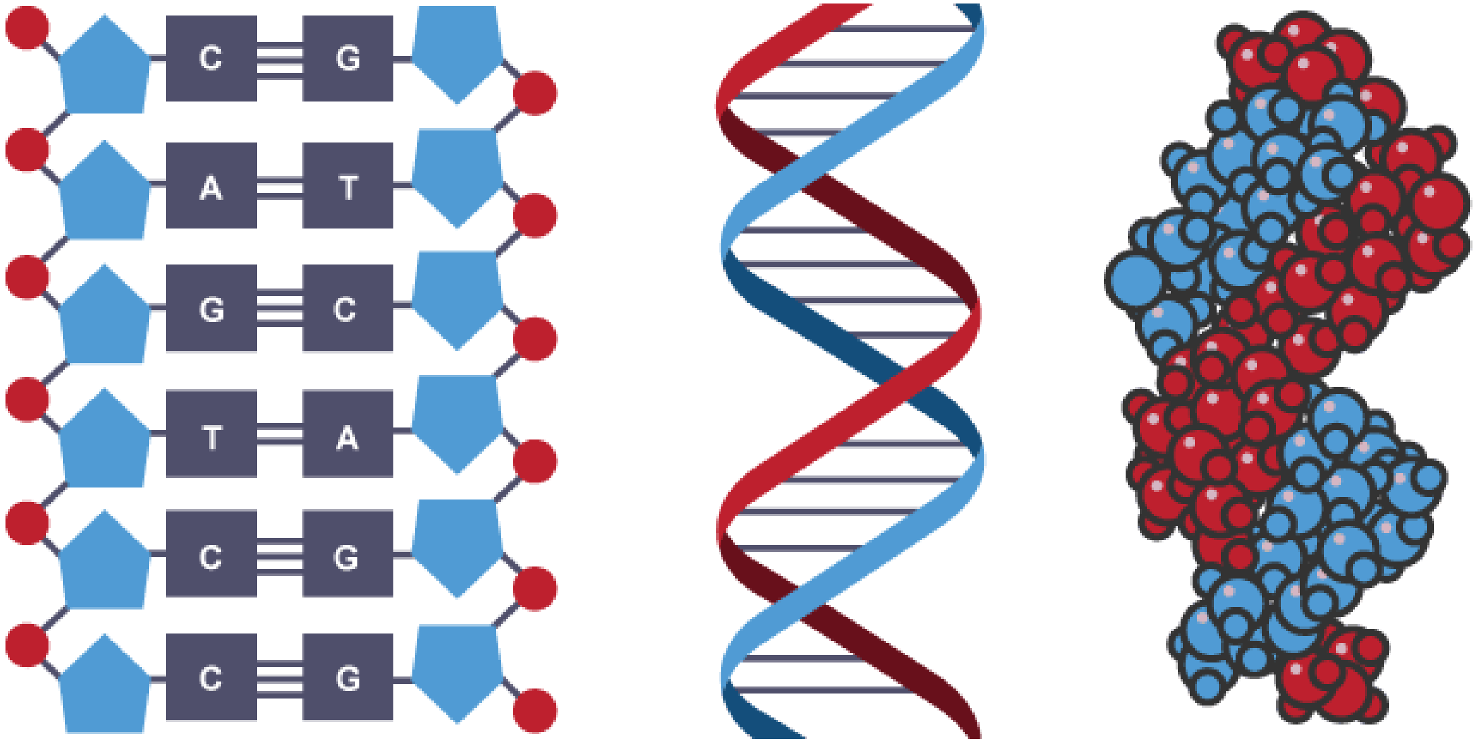

# Hamiltonian model

## Peyrard-Bishop-Dauxois (PBD) model

**[Dauxois, Peyrard, Bishop, PRE (1993)]**

$$H_N = \sum_{n=1}^{N} \left[ \frac{1}{2m} p_n^2 + D_n (e^{-a_n y_n} - 1)^2 + \frac{K}{2} (1 + \rho e^{-b(y_n + y_{n-1})})(y_n - y_{n-1})^2 \right]$$

**Bond potential energy (Morse potential)**

**GC: D=0.075 eV, a=6.9 Å$^{-1}$**

**AT: D=0.05 eV, a=4.2 Å$^{-1}$**

**Nearest neighbors coupling potential**

**K=0.025 eV/Å$^2$, ρ=2, b=0.35 Å$^{-1}$**

# Disorder realizations

**Different arrangements of AT and GC bonds.**


**$P_{AT}$=100% AT bonds**

# Disorder realizations

**Different arrangements of AT and GC bonds.**

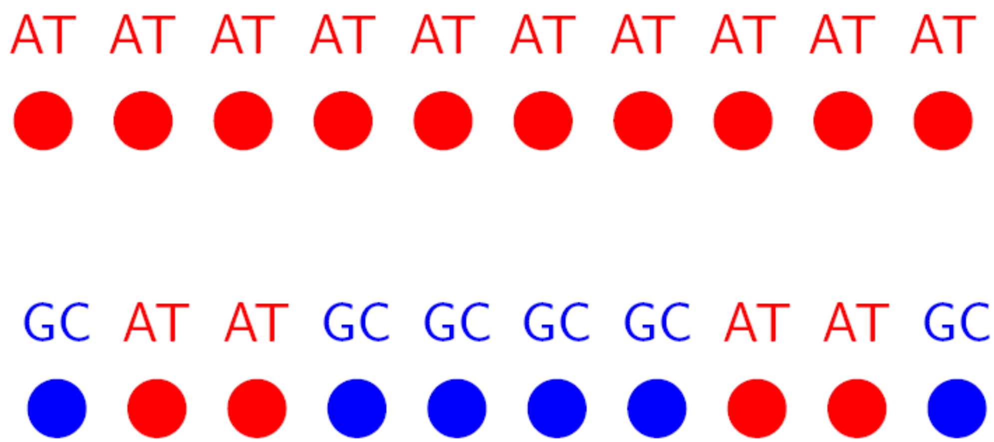


**$P_{AT}$=100% AT bonds**

**$P_{AT}$=40% AT bonds**

# Disorder realizations

**Different arrangements of AT and GC bonds.**

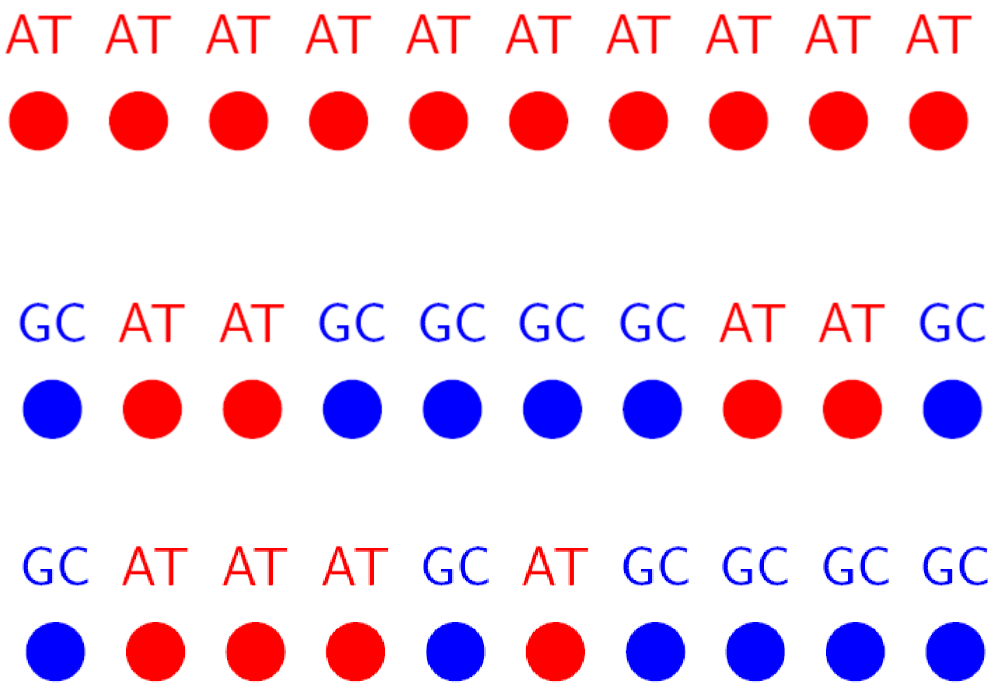


**$P_{AT}$=100% AT bonds**

**$P_{AT}$=40% AT bonds**

# Disorder realizations

**Different arrangements of AT and GC bonds.**

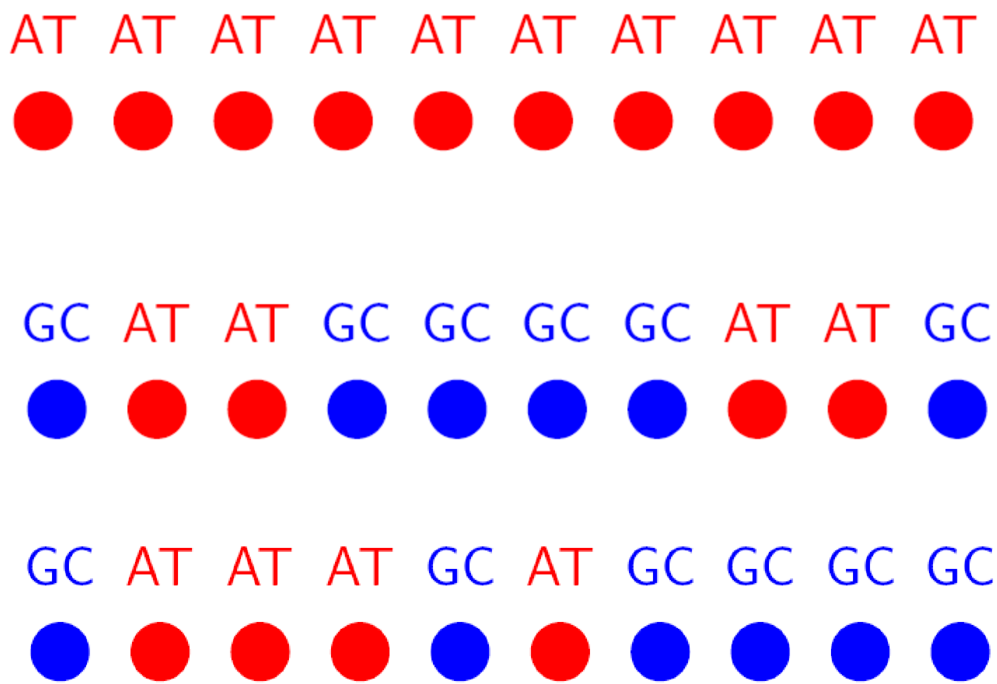


**$P_{AT}$=100% AT bonds**

**$P_{AT}$=40% AT bonds**

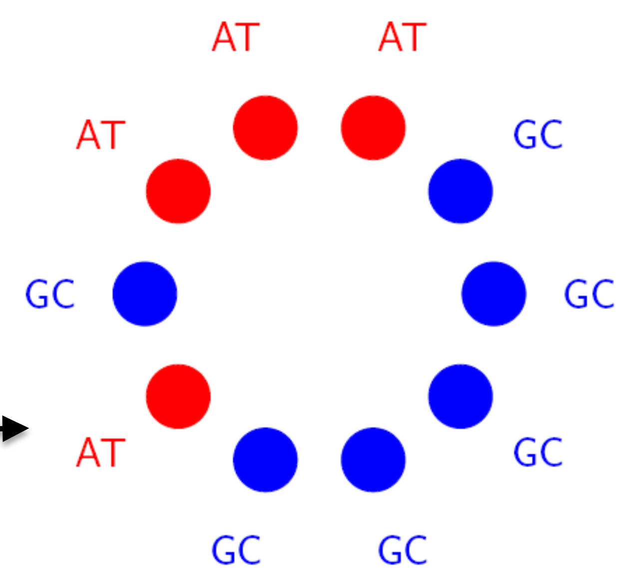


**Periodic boundary conditions**

# Lyapunov exponents (E/n=0.04, $P_{AT}$=30%)

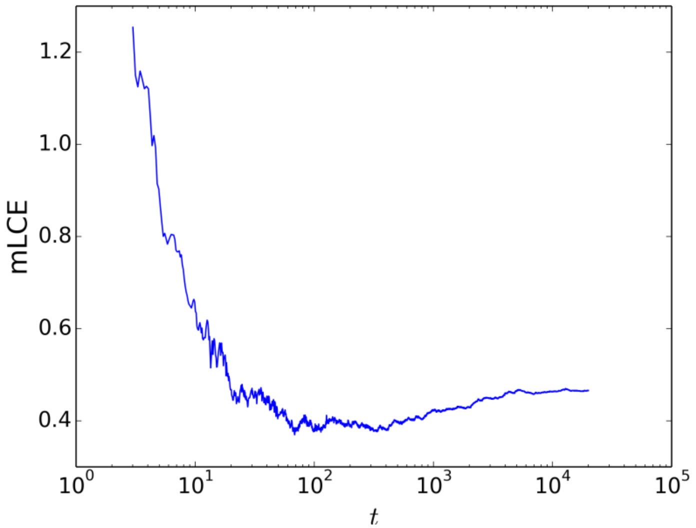


**1 realization, 1 initial condition**

# Lyapunov exponents (E/n=0.04, $P_{AT}$=30%)

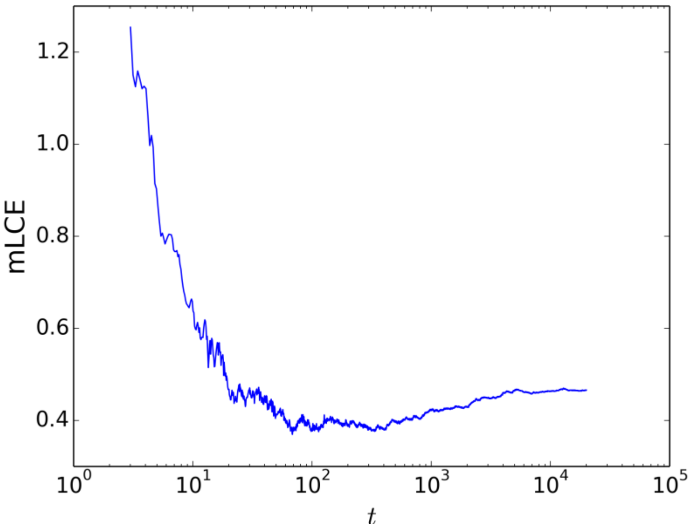


**1 realization, 1 initial condition**

**1 realization, 10 initial conditions**

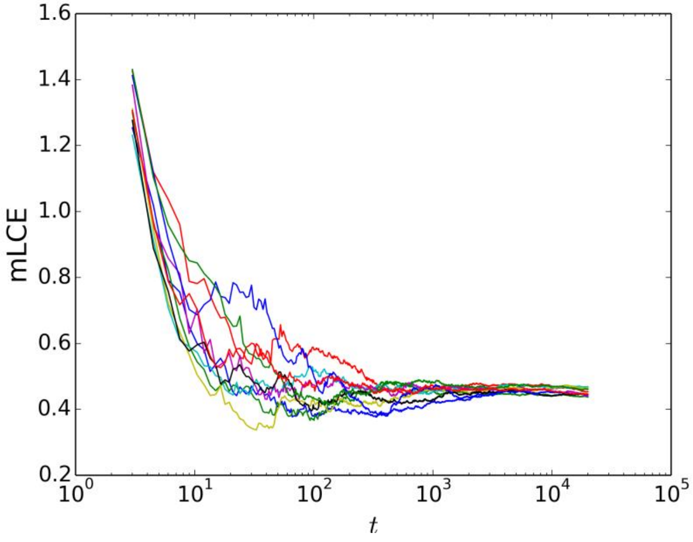

# Lyapunov exponents (E/n=0.04, $P_{AT}$=30%)

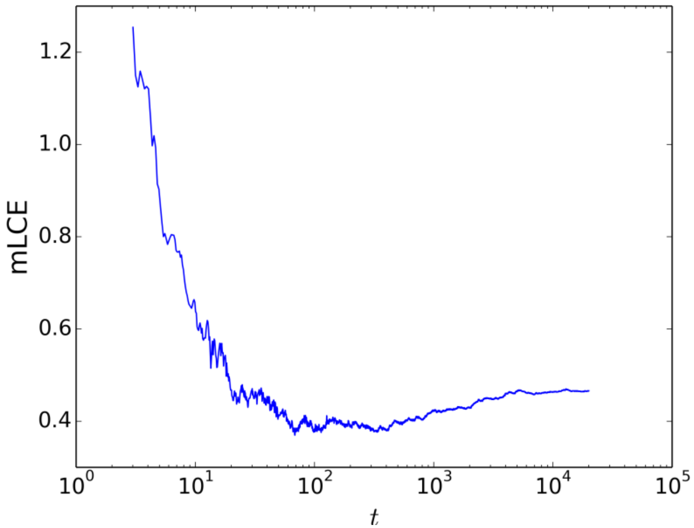


**1 realization, 1 initial condition**

**1 realization, 10 initial conditions**

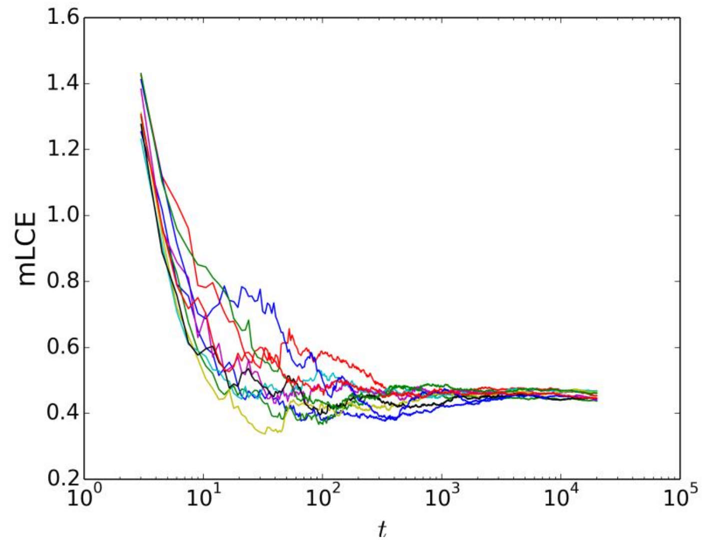


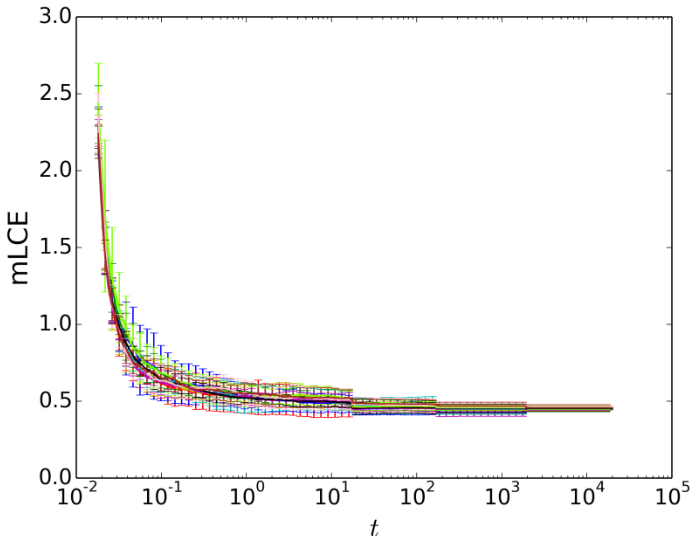


**10 realizations, 10 initial conditions**

# Lyapunov exponent vs. energy per particle

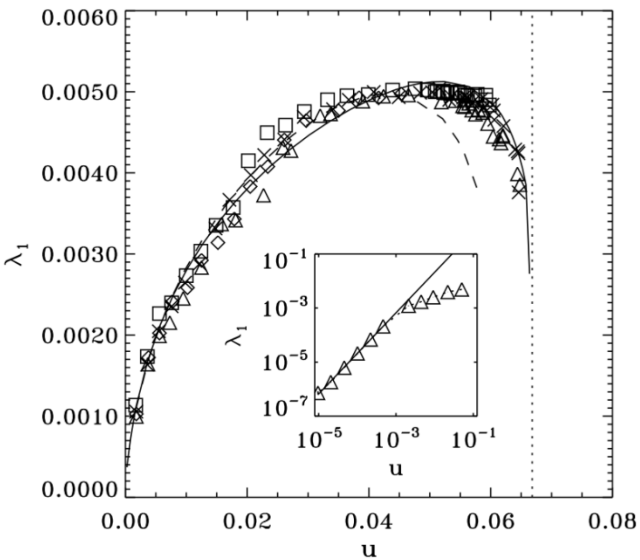


**Homogeneous chain [Barré & Dauxois, EPL (2001)]**

# Lyapunov exponent vs. energy per particle

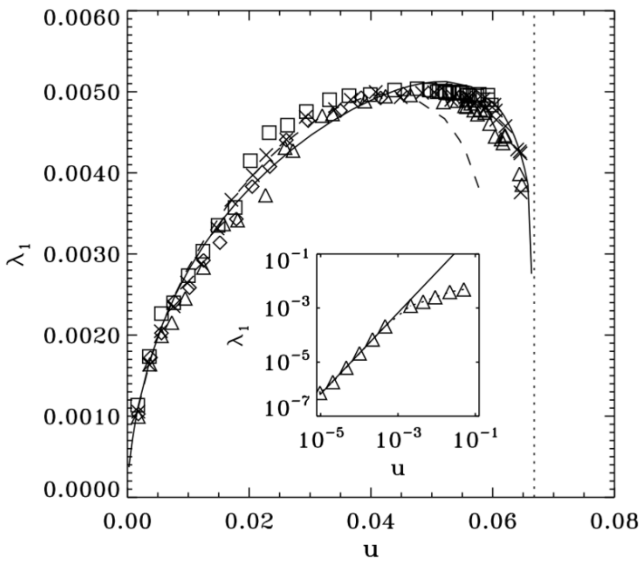


**Homogeneous chain [Barré & Dauxois, EPL (2001)]**

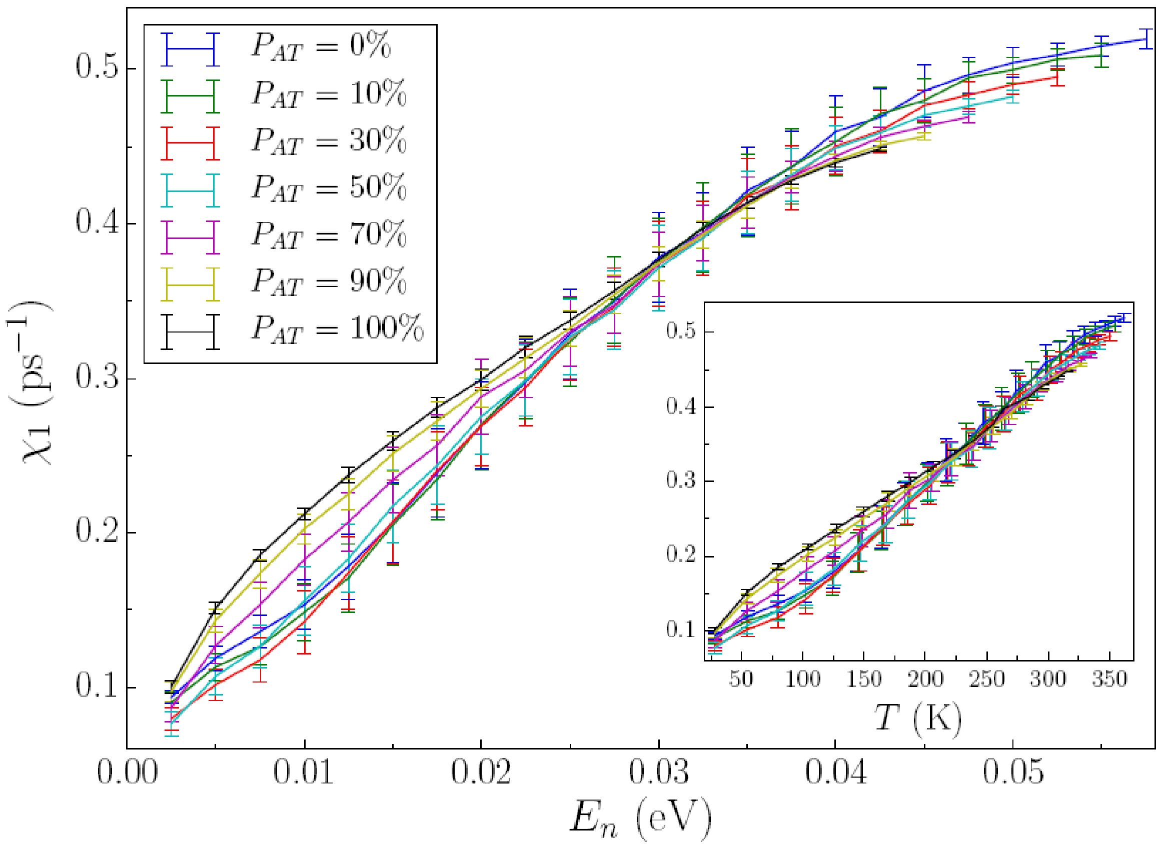

# Lyapunov exponent vs. energy per particle

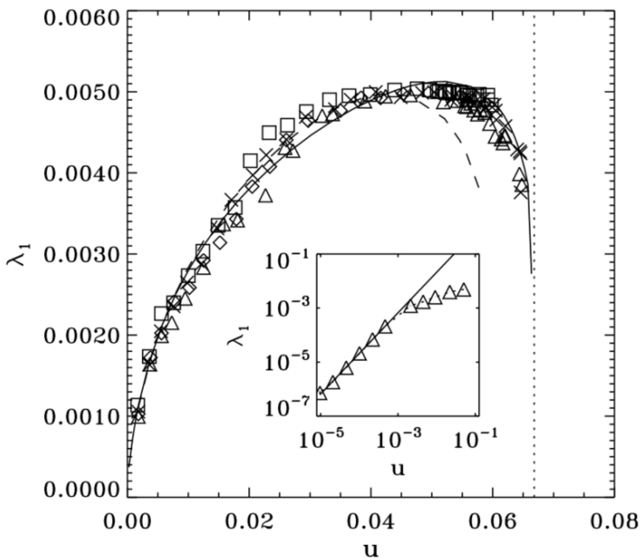


**Homogeneous chain [Barré & Dauxois, EPL (2001)]**

**GC chains more chaotic**

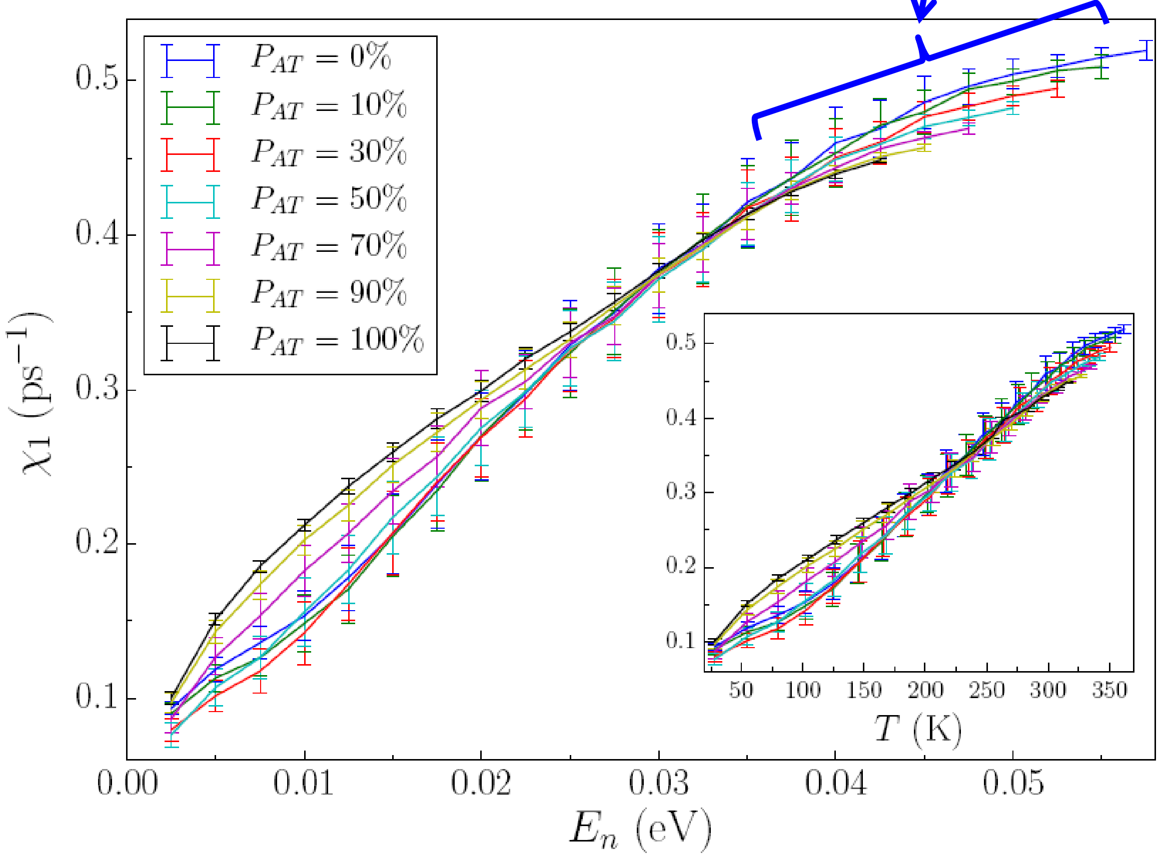

# Lyapunov exponent vs. energy per particle

AT chains
more chaotic

GC chains
more chaotic

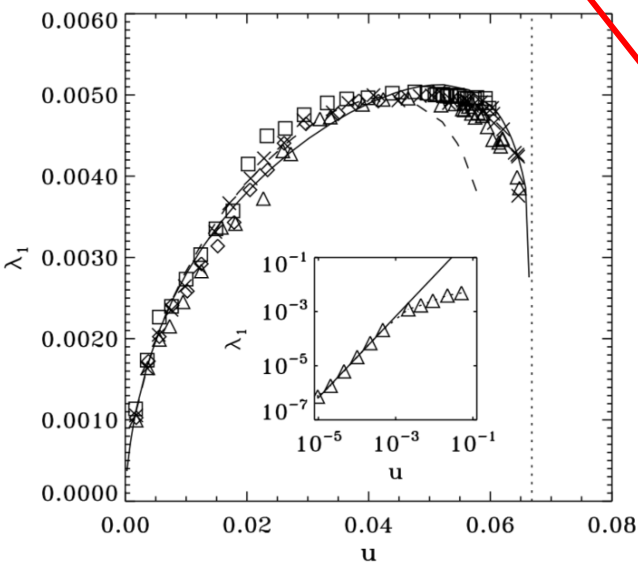


**Homogeneous chain [Barré & Dauxois, EPL (2001)]**

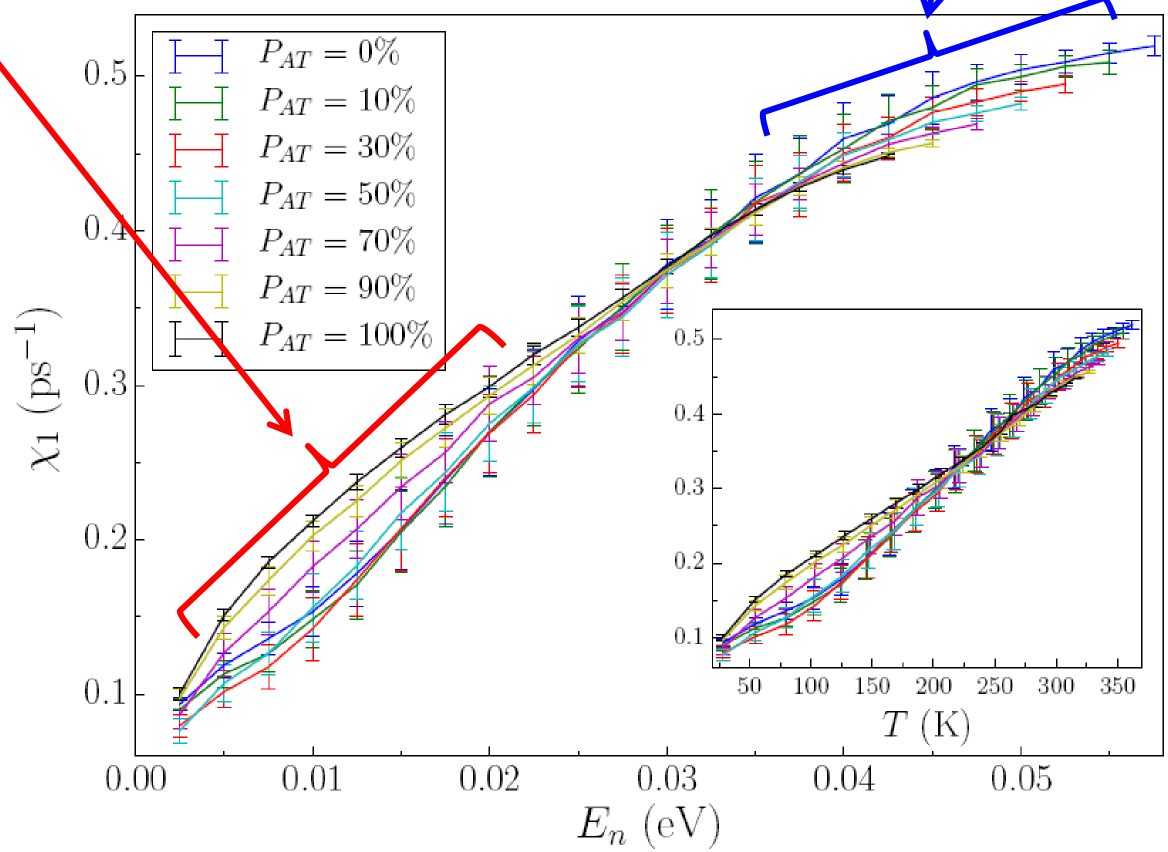

# Lyapunov exponent vs. energy per particle

AT chains
more chaotic

Type of chain
does not play
a role

GC chains
more chaotic

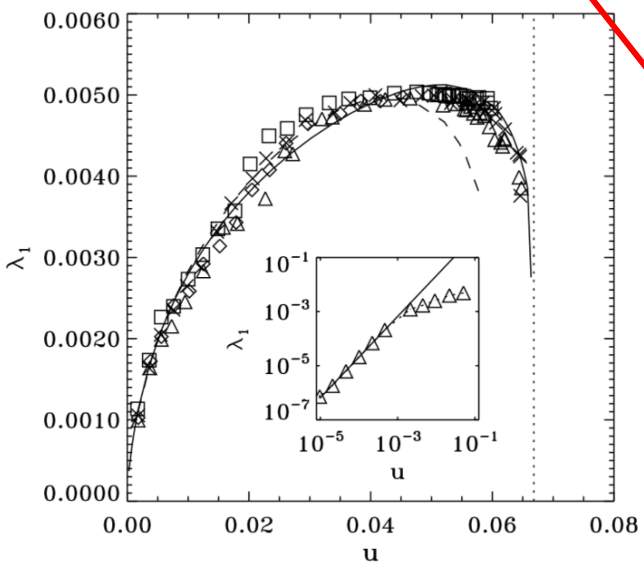


Homogeneous chain
[Barré & Dauxois,
EPL (2001)]

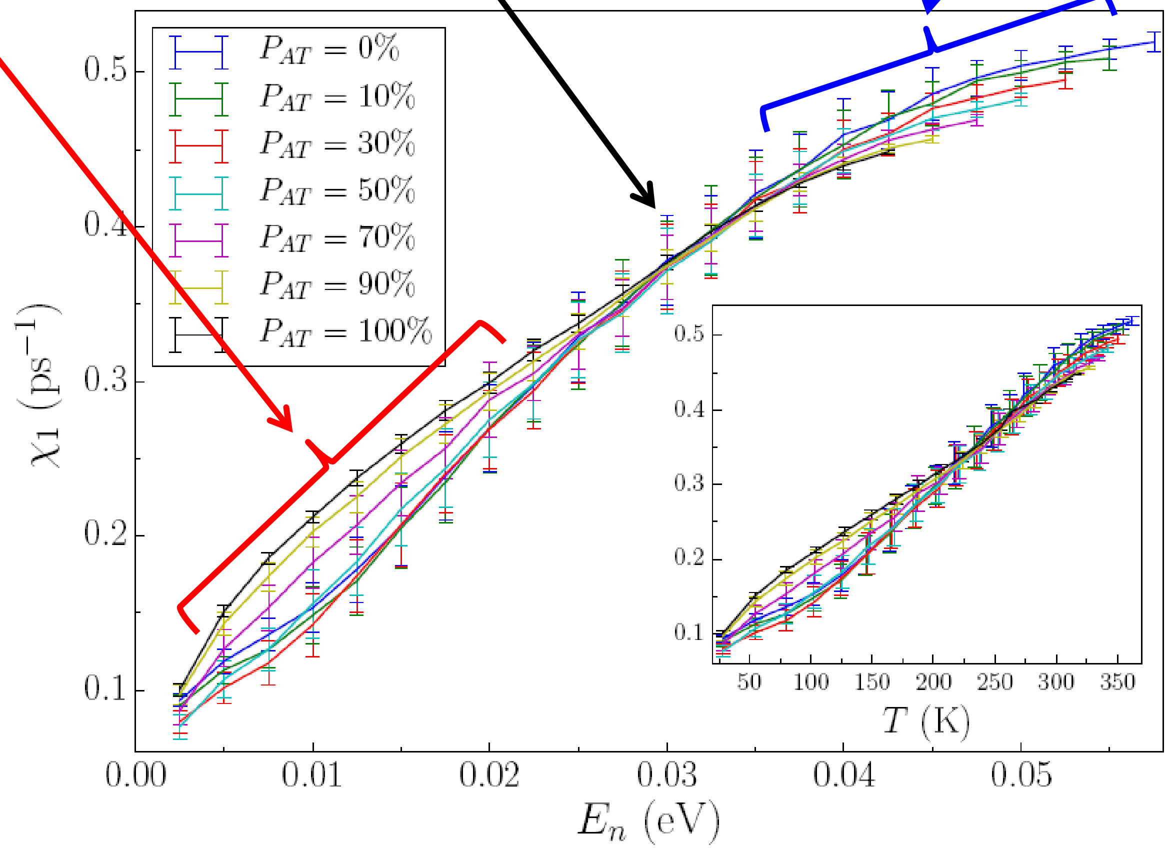

# DNA denaturation (melting)

**Melting: large bubbles forming in the DNA chain as bonds break**

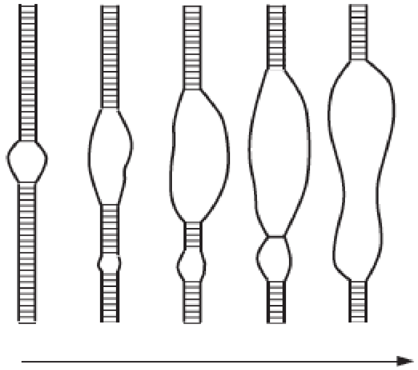


**As $y_n$ increases the exponentials in**

$$D_n(e^{-a_n y_n} - 1)^2 + \frac{K}{2}(1 + \rho e^{-b(y_n+y_{n-1})})(y_n - y_{n-1})^2$$

**tend to 0, the system becomes effectively linear and the mLCE →0.**

**$P_{AT}$=90%**
**E/n=0.085**

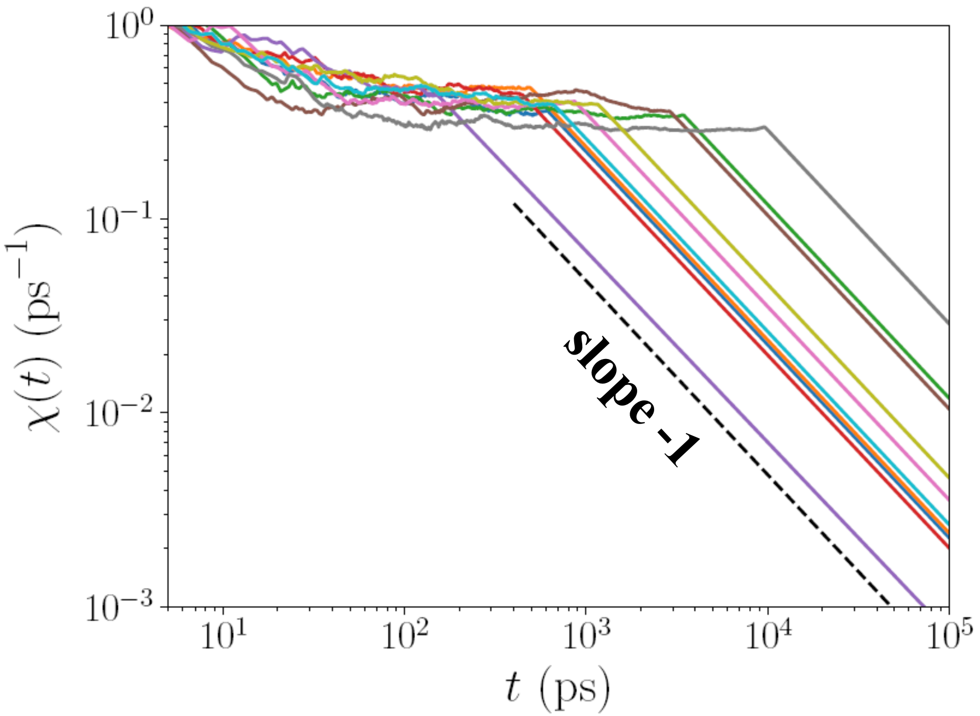

# Evolution of DVDs – Low energies

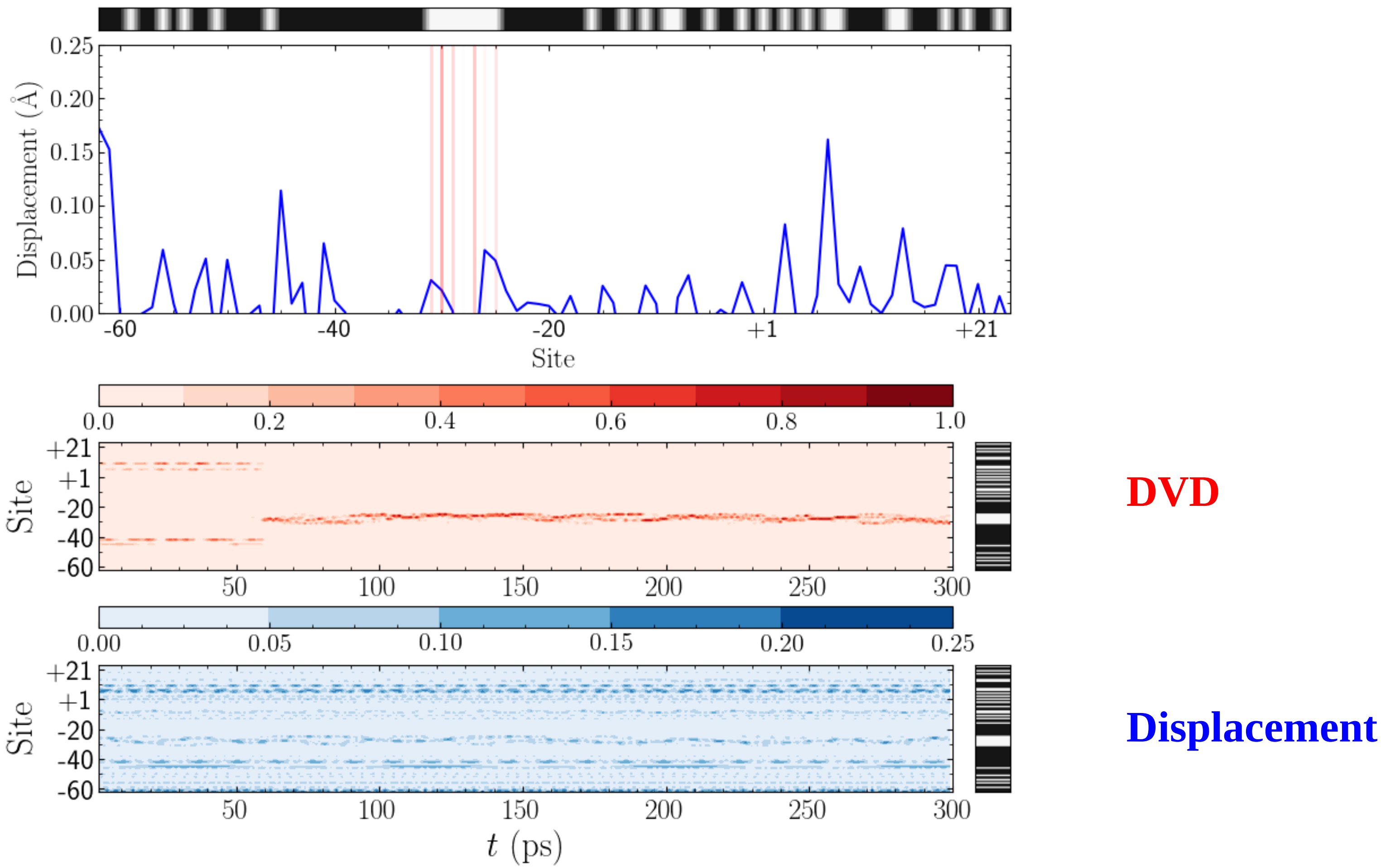


**Adenovirus major late promoter (AdMLP): 86 base pairs, $P_{AT}$=33.7%**
**E/n=0.005 eV**

# Evolution of DVDs – Higher energies

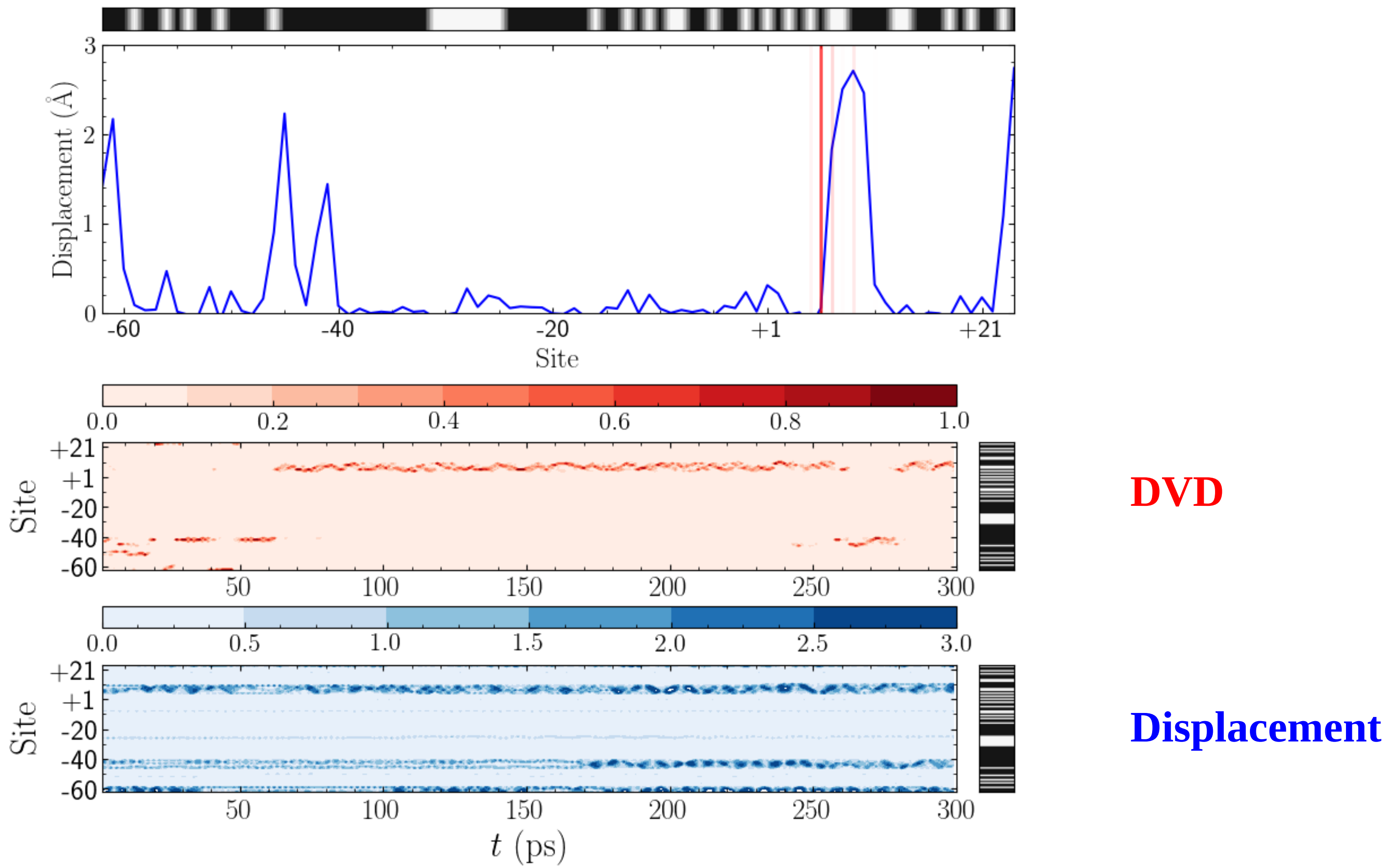


**Adenovirus major late promoter (AdMLP): 86 base pairs, $P_{AT}$=33.7%**

**E/n=0.04 eV**

# Mixing of the DNA chain

**Mixing parameter α = Number of alternations in the chain (AT and GC).**

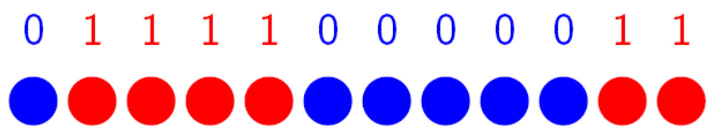


**α=4**

$$(1)\bar{0}111\bar{1}0000\bar{0}1\bar{1}(0)$$

# Mixing of the DNA chain

**Mixing parameter $\alpha$ = Number of alternations in the chain (AT and GC).**

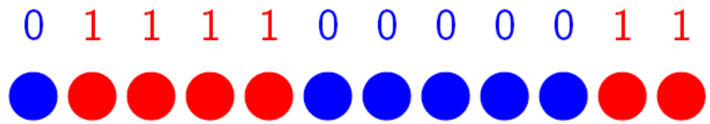


**$\alpha$=4**

$$(1)\bar{0}111\bar{1}0000\bar{0}1\bar{1}(0)$$

**Example case: N=10, $N_{AT}$=4, $N_{GC}$=6.**

**Extreme cases: $\alpha$=2 and $\alpha$=8**

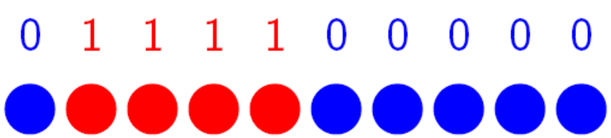


$\alpha = 2$

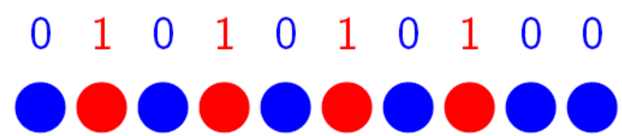


$\alpha = 8$

# Mixing of the DNA chain

**Mixing parameter α = Number of alternations in the chain (AT and GC).**

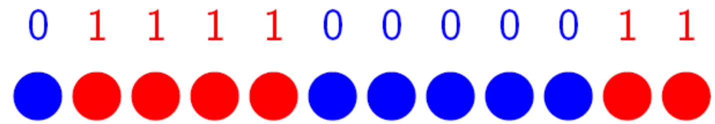


**α=4**

$$(1)\bar{0}111\bar{1}0000\bar{0}1\bar{1}(0)$$

**Example case: N=10, $N_{AT}$=4, $N_{GC}$=6.**

**Extreme cases: α=2 and α=8**

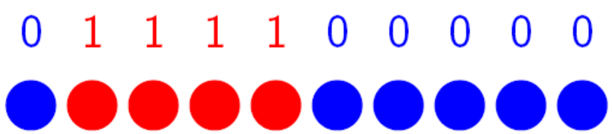


$\alpha = 2$

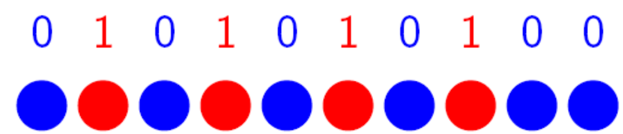


$\alpha = 8$

$$\boxed{2 \leq \alpha \leq \min\{2N_{AT}, 2N_{GC}\}, \quad \alpha \text{ even}}$$

# Effect of mixing

Probability distribution function P(α)

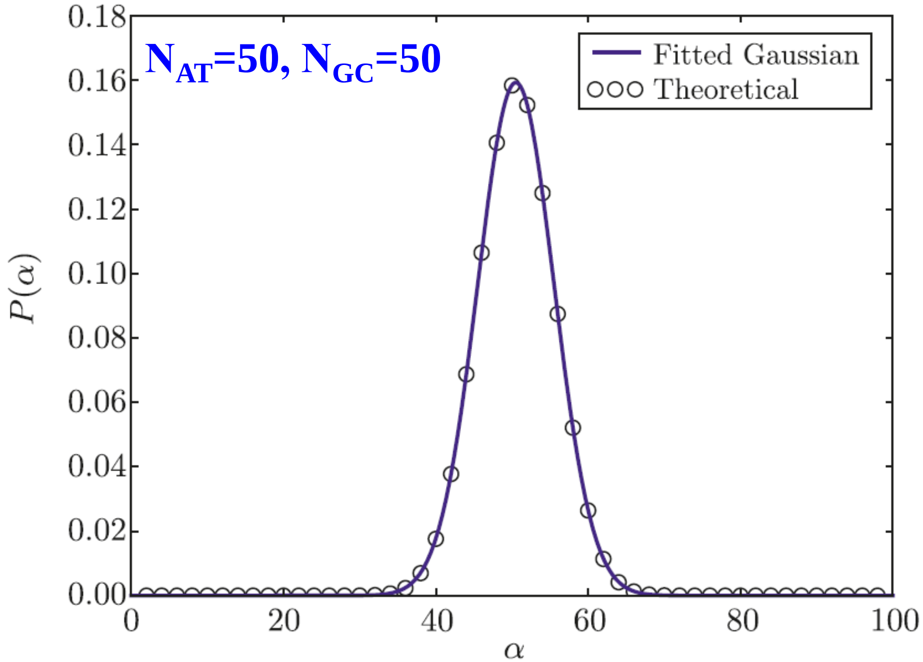


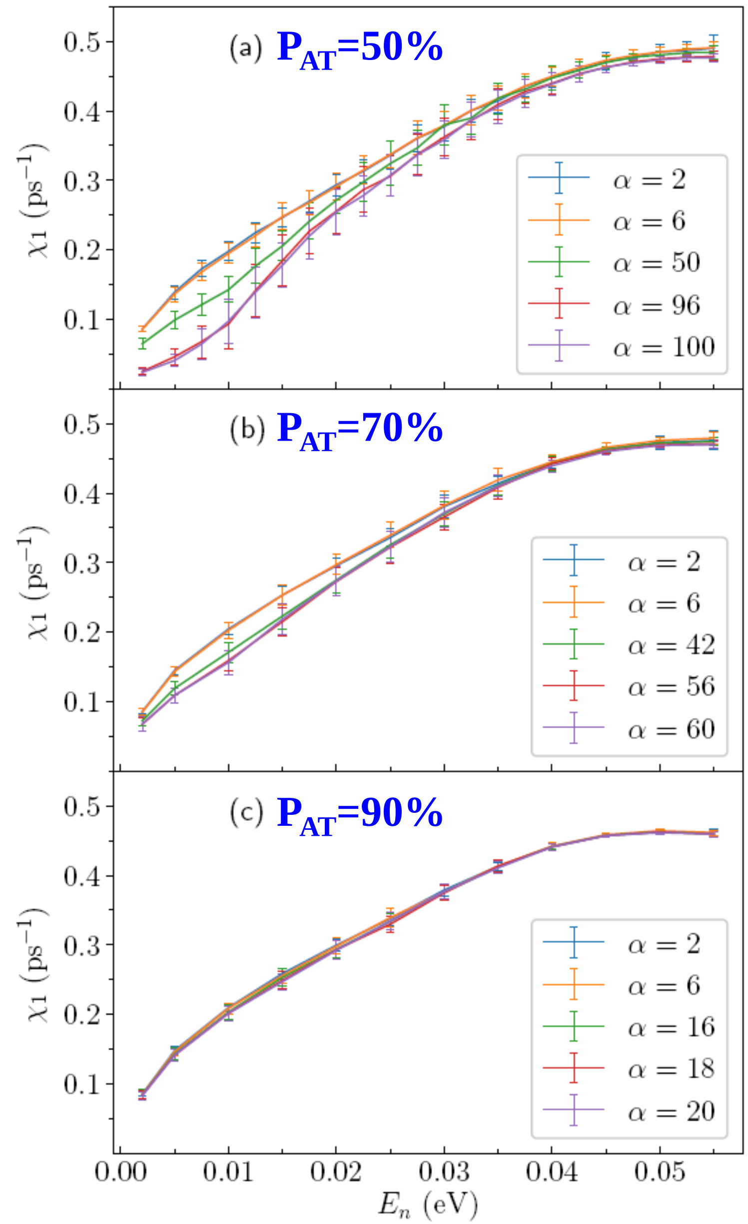


**In chains not dominated by a single base-pair type:**
**More homogeneous chains (large values of α) are less chaotic**

# Future works

- DKG and DDNLS models in 2 spatial dimensions
- Extended, sequence-dependent PBD models of DNA
- More complicated models of granular material
- Graphene models

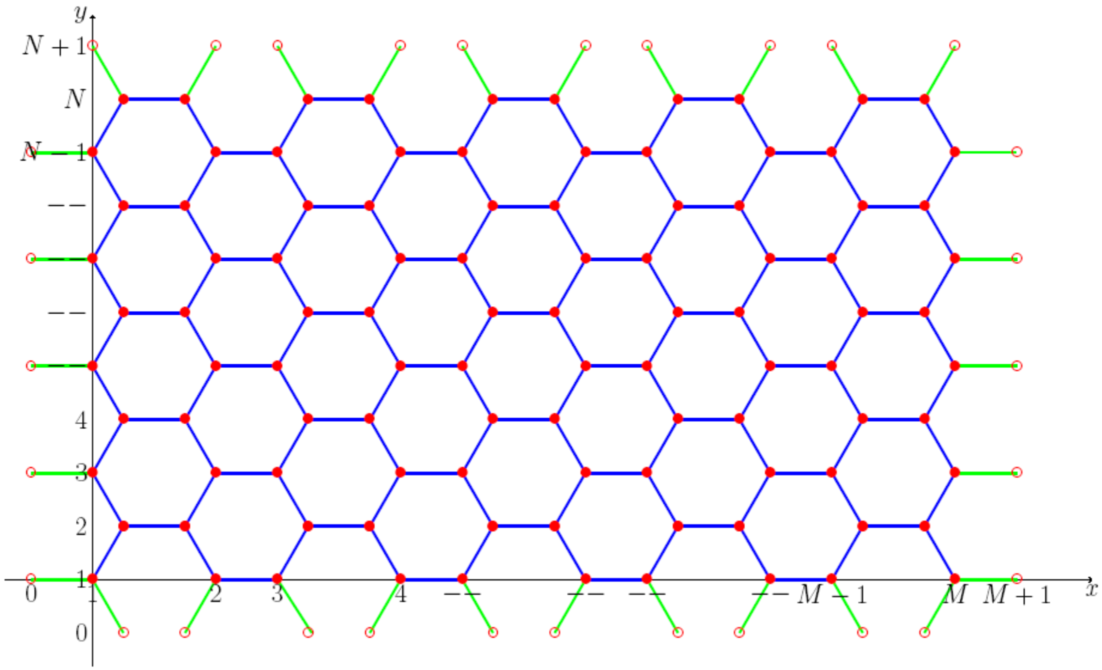

# Future works

## DDNLS in 2 spatial dimensions (strong chaos)

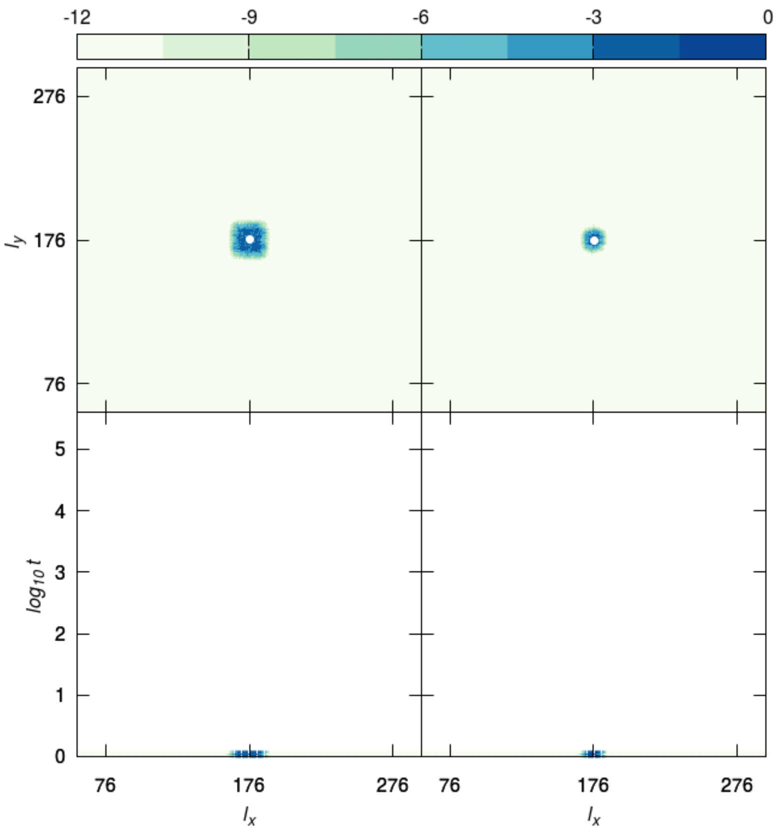


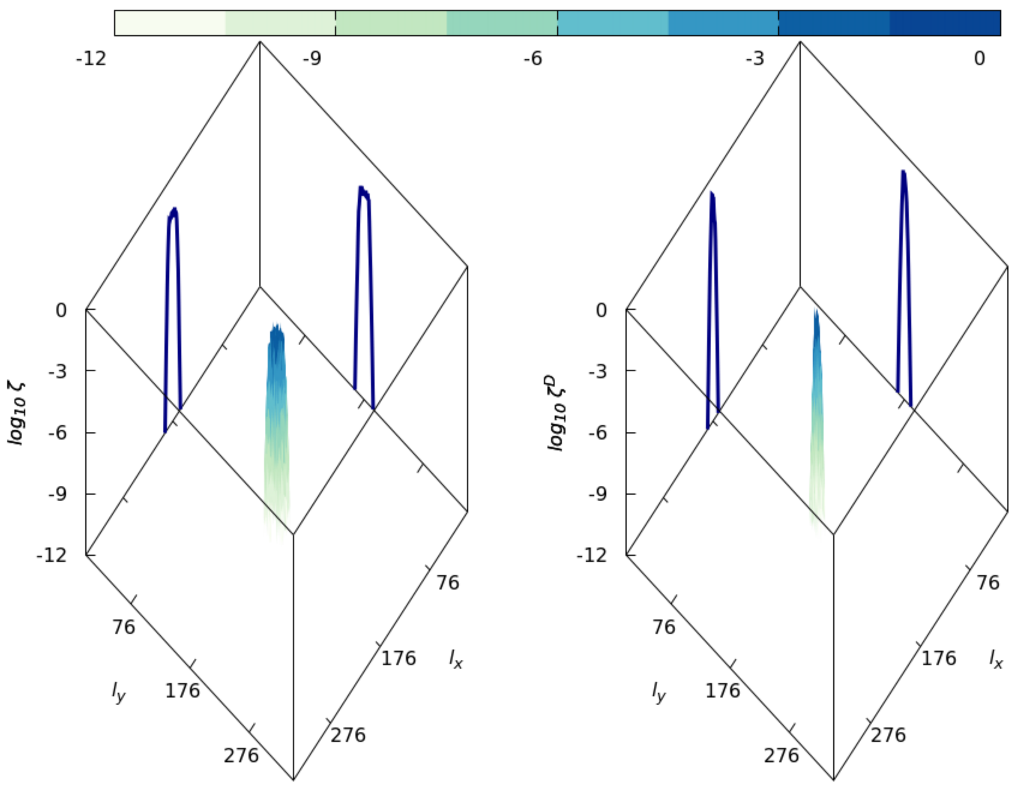


**Norm** **DVD** **Norm** **DVD**

# Future works

## DDNLS in 2 spatial dimensions (strong chaos)

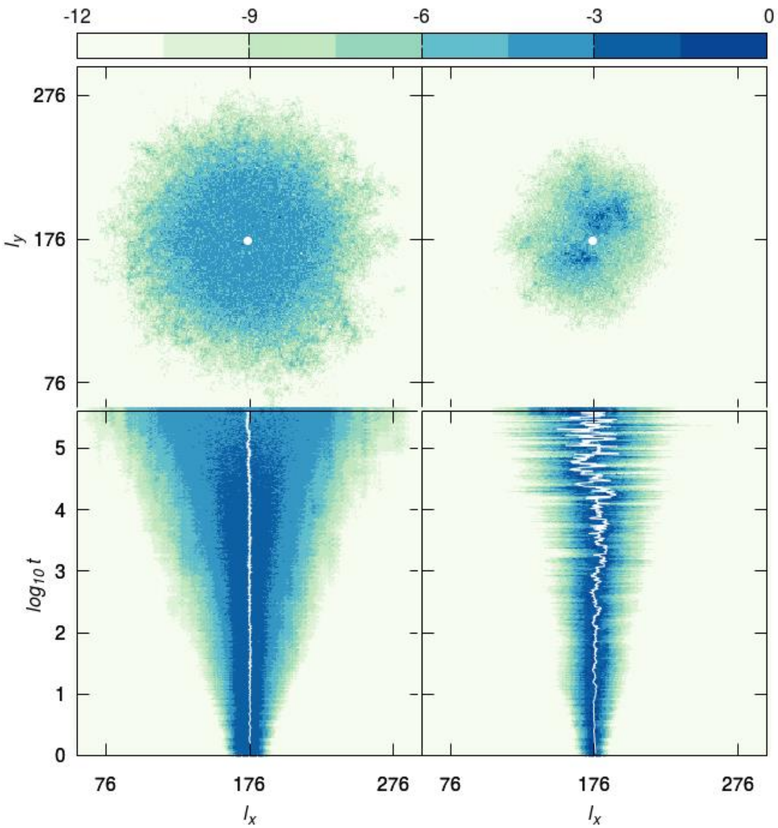


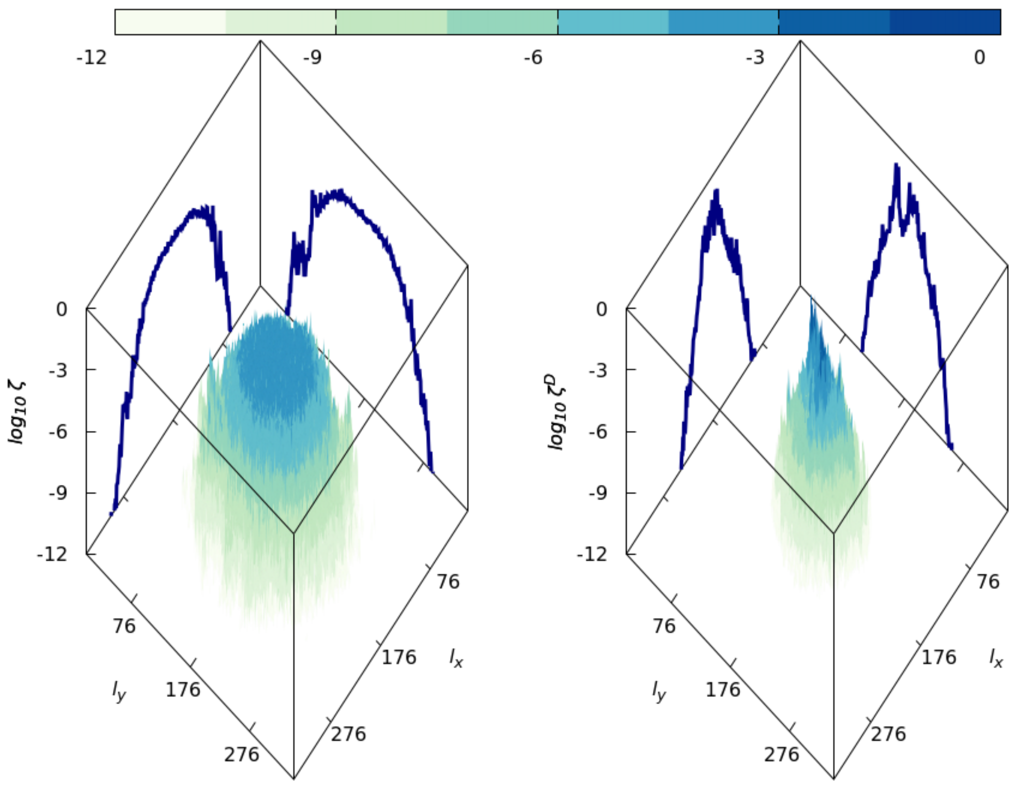


**Norm** **DVD** **Norm** **DVD**

# Summary I

- **Both the DKG and the DDNLS models show similar chaotic behaviors**
- **The mLCE and the DVDs show different behaviors for the weak and the strong chaos regimes.**
- **Lyapunov exponent computations show that:**
  - ✓ **Chaos not only exists, but also persists.**
  - ✓ **Slowing down of chaos does not cross over to regular dynamics.**
  - ✓ **Weak chaos: mLCE ~ $t^{-0.25}$ - Strong chaos: mLCE ~ $t^{-0.3}$**
- **The behavior of DVDs can provide information about the chaoticity of a dynamical system.**
  - ✓ **Chaotic hot spots meander through the system, supporting a homogeneity of chaos inside the wave packet.**

**B. Senyange, B. Many Manda & Ch. S.: Phys. Rev. E, 98, 052229 (2018) 'Characteristics of chaos evolution in one-dimensional disordered nonlinear lattices'**

# Summary II

- **Chaotic dynamics of granular chains**
  - ✓ **Weakly nonlinear regime: although the overall system behaves chaotically, it can exhibit long-lived chaotic Anderson-like localization for particular single particle excitations.**
  - ✓ **Highly nonlinear regime: the granular chain reaches energy equipartition and an equilibrium chaotic state, independent of the initial position excitation.**
  - ✓ **The discontinuous nonlinearity (gaps) triggers chaos in the Hertzian model, while the propagation of gaps leads to equipartition.**
  - ✓ **The FPUT system exhibits an alternate behavior between localized and delocalized chaotic behavior which is strongly dependent on the initial energy excitation.**

**V. Achilleos, G. Theocharis & Ch. S.: Phys. Rev. E, 97, 042220 (2018) 'Chaos and Anderson-like localization in polydisperse granular chains'.**

**A. Ngapasare, G. Theocharis, O. Richoux, Ch. S. & V. Achilleos: Phys. Rev. E, 99, 032211 (2019) 'Chaos and Anderson localization in disordered classical chains: Hertzian versus Fermi-Pasta-Ulam-Tsingou models'.**

# Summary III

- **Heterogeneity influences the chaotic behavior of the DNA chaotic behavior.**
- **Behavior of the DVD:**
  - ✓ **It is always quite localized**
  - ✓ **For small energies  tends to be concentrated in larger homogenous parts of the chain**
  - ✓ **For larger energies jumps, with no apparent pattern, between sites next to a relative large displacement.**
- **Alternation index affects the mLCE in chains not dominated by a single base-pair type: More homogeneous chains (large values of α) are less chaotic, for small energies.**

**M. Hillebrand, G. Kalosakas, A. Schwellnus & Ch. S.: Phys. Rev. E, 99, 022213 (2019)**
**'Heterogeneity and chaos in the Peyrard-Bishop-Dauxois DNA model '**

# References


- Flach, Krimer, S. (2009) PRL, 102, 024101
- S., Krimer, Komineas, Flach (2009) PRE, 79, 056211
- S., Flach (2010) PRE, 82, 016208
- Laptyeva, Bodyfelt, Krimer, S., Flach (2010) EPL, 91, 30001
- Bodyfelt, Laptyeva, S., Krimer, Flach (2011) PRE, 84, 016205
- Bodyfelt, Laptyeva, Gligoric, S., Krimer, Flach (2011) IJBC, 21, 2107
- S., Gkolias, Flach (2013) PRL, 111, 064101
- Tieleman, S., Lazarides (2014) EPL, 105, 20001
- Antonopoulos, Bountis, S., Drossos (2014) Chaos, 24, 024405
- Antonopoulos, S., Bountis, Flach (2017) Chaos Sol. Fract., 104, 129
- Senyange, Many Manda, S. (2018) PRE, 98, 052229


**DKG and DDNLS models**


- S., Gerlach (2010) PRE, 82, 036704
- Gerlach, S. (2011) Discr. Cont. Dyn. Sys.-Supp., 2011, 475
- Gerlach, Eggl, S. (2012) IJBC, 22, 1250216
- S., Gerlach, Bodyfelt, Papamikos, Eggl (2014) Phys. Lett. A, 378, 1809
- Gerlach, Meichsner, S. (2016) Eur. Phys. J. Sp. Top., 225, 1103
- Senyange, S. (2018) Eur. Phys. J. Sp. Top., 227, 625
- Danieli, Many Manda, Mithun, S. (2019) MinE, 1, 447


**Symplectic integrators and 'Tangent Map' method**


- Achilleos, Theocharis, S. (2016) PRE, 93, 022903
- Achilleos, Theocharis, S. (2018) PRE, 97, 042220
- Ngapasare, Theocharis, Richoux, S., Achilleos (2019) PRE, 99, 032211


**Granular chains**


- Hillebrand, Paterson-Jones, Kalosakas, S. (2018) Reg. Chaotic Dyn., 23, 135
- Hillebrand, Kalosakas, Schwellnus, S. (2019) PRE, 99, 022213


**PBD model of DNA**

# Poster on chaos detection in Hamiltonian lattices

## Investigating Chaos by the Generalized Alignment Index (GALI) Method

Henok Moges and Haris Skokos
University of Cape Town, Cape Town, South Africa

**Henok Moges**